

1 **Differential invariant signatures for planar Lie group transformations of images**

2 Richard Brown, Stephen Marsland, and Robert McLachlan

3

4 **Abstract.** Changes in viewpoint, such as camera motion, impose transformations on the objects in an im-
5 age, and these transformations will differ for objects at different positions relative to the camera.
6 Typically these transformations will be elements of planar Lie groups. While there have been signif-
7 icant advances in object recognition using machine learning in recent years, the question of how to
8 recognise an object in an image as its appearance varies through camera motion and similar effects
9 remains open. We demonstrate how differential invariant signatures can be derived for each of the
10 transformation groups, and how the underlying invariances reflect the group-subgroup structure of
11 the transformation groups.

12 There are a variety of methods that can be used to identify differential invariants, and we provide examples
13 of three of them: tensor contraction, transvectants, and the method of moving frames. We use the resulting
14 invariants to construct practical sets to form three-dimensional invariant signatures. These signatures are not
15 necessarily complete: the image cannot always be reconstructed uniquely up to transformation, but they are
16 plottable, and depend at worst on third derivatives, although more channels of information, such as colour im-
17 ages, can reduce the highest order of derivative needed in some cases. We demonstrate the invariant signatures
18 for each transformation group based on a simple smooth image. A full consideration of how these signatures
19 could be used in practice will require effective methods to numerically approximate derivatives for images.

20 **Key words.** Object recognition, planar transformation, planar Lie groups, invariants, differential invariant sig-
21 nature

22 **AMS subject classifications.** 65D18, 53A55, 68U10

23 **1. Introduction.** The appearance of a fixed object in a set of images can vary markedly
24 depending upon such variables as pose and position relative to the camera, even though the
25 object itself does not change. This is even more marked in scenes that consist of multiple
26 objects at different distances and orientations to the camera against a fixed background. The
27 appearance of each individual object will then vary independently as a constant camera motion
28 or other such transformation is applied. Typically the individual transformations will appear
29 as the action of an element of a planar Lie group, for example the affine, or projective groups,
30 or an angle-preserving transformation from the conformal group, depending upon the camera
31 model.

32 For image recognition it is then natural to seek representations of objects that do not
33 change as these various transformation groups act. If the space of objects is denoted M and
34 the appearance transformations form a group \mathcal{G} , then mathematically one seeks a way to
35 study objects in M/\mathcal{G} . One way to achieve this is by transforming all objects to match a
36 chosen target object by registration (the transformation of the appearance of one shape to
37 match another, typically by gradient descent on a matching function, see e.g., [Modersitzki,
38 2003]). For example, for the group of similarity transformations (rotation and reflection,
39 translation, and scale), a Procrustes alignment [Kendall, 1989] will place all of the shapes
40 into the reference frame of one template example. However, analysis on these quotient spaces
41 is rarely simple (see e.g., Pennec et al. [2019] for a basic primer), and if one is interested in
42 the object, and not the transformation, then it necessitates a lot of computational work for

43 relatively little benefit. The alternative approach, of showing examples of each object after
44 applying sufficiently many transformations that the classifier can learn to recognise the object
45 after any group transformation, inevitably scales extremely badly.

46 An alternative option is to seek \mathcal{G} -invariant functions on M . Mathematical invariants
47 provide a useful way to identify sets of objects that are the same up to some equivalence
48 relation, since the functions are constant for objects in the same equivalence class (orbits of
49 the group). For images, rather than considering the image of the object, one constructs an
50 invariant signature of some kind, which represents the object modulo the action of elements
51 from the relevant group. This has been considered extensively by Olver and co-authors for
52 the case of outlines of objects [Calabi et al., 1998, Hoff and Olver, 2013]. We extend this by
53 considering the case of signatures for images rather than outlines of curves under a variety of
54 transformation groups of relevance to image analysis.

55 A greyscale image can be viewed as a two-dimensional manifold embedded in a three
56 dimensional ambient space, with coordinates $(x, y, f(x, y))$. A signature $\mathcal{I}(f) \in \mathbb{R}^m$ has coor-
57 dinates $\mathcal{I}(f) = (I_1, I_2, \dots, I_m)$, where each I_i is a function of $f(x, y)$ and its derivatives, and
58 will therefore be a two-dimensional manifold embedded in \mathbb{R}^m . Under a change of coordinates
59 $(x, y) \mapsto (\bar{x}, \bar{y})$ induced by a group action, the signatures of the original image and transformed
60 version $\bar{f}(\bar{x}, \bar{y}) = f(x, y)$ will be the same. The introduction of an invariant signature reduces
61 the object recognition problem modulo some transformation group to one of comparing the
62 signatures of the objects, rather than the images themselves. We do not consider the question
63 of classification further in this paper; a standard image recognition algorithm can be used
64 (see, e.g., Zhang et al. [2020] for a survey), or a matching method such as Benn et al. [2019]
65 can be used.

66 Ideally, an invariant signature would be complete, so that the image is exactly determined
67 by the signature up to a transformation, and two objects share a signature if and only if
68 they differ only by a transformation from \mathcal{G} . However, there are some pathological scenarios
69 that occur regularly in images, particularly that flat regions of images collapse down to single
70 points in the signature (as all of the derivatives are zero in these regions). Then images that
71 are otherwise similar (apart from the size of one of these regions) cannot be distinguished.
72 However, the number of dimensions m of the ambient manifold can increase markedly for
73 complete signatures, increasing the computational cost and making it impossible to visualise
74 the signature surface. For many applications an incomplete signature is sufficient, and is what
75 we consider here, favouring signatures in three coordinates, since for greyscale images, \mathbb{R}^3 is
76 the smallest space in which the signature surfaces can reside. If the signature is not complete,
77 then there will be a ‘bad set’ of images that cannot be distinguished from each other. The
78 codimension of the bad set is defined as the difference between the dimensionalities of the
79 whole space and of the bad set. The codimension should ideally be large, meaning that the
80 dimension of the bad set would be small.

81 In addition to a bad set of high codimension, in order for the invariant signatures to be
82 useful to identify similarity in images, there are two other key considerations: they must vary
83 continuously with respect to the image, and they must be robust with respect to occlusions,
84 where one object obscures some part of another. These constraints are essential if the signature
85 is to be used to detect similarity of images, but the first fails for the rational invariants found
86 in the literature. Such considerations lead one naturally to consider local invariants, i.e., those

87 defined using each point of the object as its own basepoint, together with a neighbourhood
88 in some topology. This is sufficient to compute, e.g., derivatives of an object. For this reason
89 we focus on differential invariants. The disadvantage of such invariants, as we shall discuss,
90 is the need to compute several orders of spatial derivative of the image. See [Marsland and](#)
91 [McLachlan \[2016\]](#) and references therein for more discussion about the desirable properties of
92 a set of invariants for image and curve analysis.

93 In this paper our aim is develop the mathematical underpinnings of constructing differen-
94 tial invariant signatures for images under the action of planar Lie groups, and to summarise
95 the impediments to a practical implementation, including the number of derivatives required.
96 We demonstrate three distinct methods of computing differential invariants: by tensor con-
97 traction, using the theory of transvectants, and via the method of moving frames, applying
98 the methods to a variety of the planar Lie groups, providing sample signature sets for the
99 various groups we consider, together with an example of a sample signature surface based on
100 a random transformation of a simple, smooth image.

101 The set of groups that we consider are shown as a lattice in Fig. 1, where the size of the
102 groups decrease down the page, and the arrows denote the subgroup relationship. There is
103 an important relationship between a group and its subgroups for invariants, which is that
104 invariants of a group are automatically invariants of its subgroups. This means that care
105 is needed to distinguish between the two, with further invariants that are known not to be
106 invariant in the supergroup included. The finite-dimensional groups in this lattice were chosen
107 because they are the only planar Lie groups that include translation and have locally primitive
108 algebras (that is, for any open subset of the plane, there is no one-dimensional foliation that
109 is left invariant by the action of the corresponding group [\[González-López et al., 1992\]](#)).
110 This makes them the groups most directly relevant to image transformations. The infinite-
111 dimensional examples are likewise those most likely to be of interest for image transformation,
112 in particular the full diffeomorphism group, which is commonly used for image registration
113 for medical images, see e.g., [Younes \[2010\]](#).

114 **2. Preliminaries.**

115 **2.1. Concepts and Notation.** We define a *k*-colour image as a triple (f, Ω, k) where
116 $\Omega \subset \mathbb{R}^n$ (typically, images are planar, so $n = 2$), $1 \leq k \in \mathbb{Z}$ is the number of colour channels,
117 and $f: \Omega \rightarrow \mathbb{R}^k$. The function f will be taken to be as smooth as necessary. Consider a (finite
118 or infinite-dimensional) local transformation group \mathcal{G} . A transformation $\varphi \in \mathcal{G}$ acts on images
119 by $\varphi \cdot (f, \Omega, k) = (f \circ \varphi^{-1}, \varphi(\Omega), k)$. We mostly consider greyscale images, so $k = 1$. Also,
120 since we work locally, we will usually omit the domain Ω .

121 In order to define differential invariants, it is necessary to identify how the group transfor-
122 mation φ acts on derivatives of the function f via the jet space [\[Olver, 1995\]](#). The d -th order
123 jet space J^d consists of the function itself and the set of all partial derivatives of the function
124 up to order d . (Note that there are $\binom{d+k-1}{k}$ partial derivatives of order d .) As the
125 group \mathcal{G} is local, it acts naturally on derivatives of the transformation, and so each individual
126 transformation $\varphi \in \mathcal{G}$ can be prolonged to act on the jet space J^d . We can thus prolong the
127 action of the group and consider the action of \mathcal{G} on not just f , but all derivatives of f up to
128 order d . A d -th order differential invariant is then a local scalar function $I: J^d(f, \Omega, k) \rightarrow \mathbb{R}$

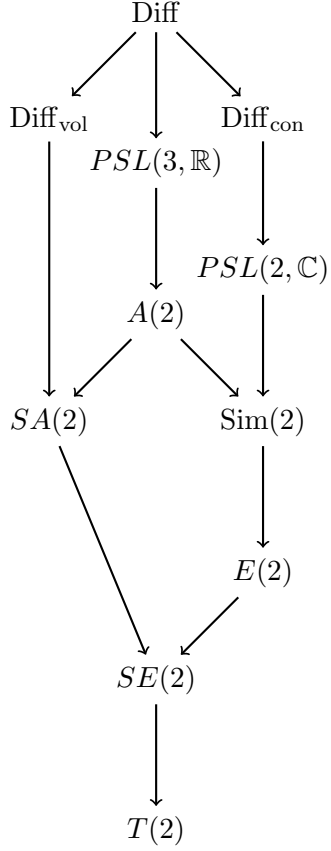


Figure 1. The lattice of groups considered in this paper. The edges identify subgroups.

129 that is invariant under the action of \mathcal{G} , i.e., $I(\varphi(f, \Omega, k)) = I(f, \Omega, k) \forall \varphi \in \mathcal{G}$. It can also be
 130 useful to consider the maximum order of derivative in the invariant, which we term degree,
 131 e.g., $f_{xy}^2 f_x f_y$ has degree 2.

132 An signature set is the image of m invariants $\mathcal{I} = (I_1, I_2, \dots, I_m)$. For simplicity of
 133 notation we will write $\mathcal{I}(f) \subset \mathbb{R}^m$ with the understanding that each signature component is
 134 actually acting on the jet space $J^d(f, \Omega, k)$. See Section 2.3 for a basic example. A signature
 135 set is complete for f if it determines f up to transformations from \mathcal{G} , i.e., if $\mathcal{I}(\tilde{f})(\tilde{\Omega}) = \mathcal{I}(f)(\Omega)$
 136 implies that there exists a transformation $\varphi \in \mathcal{G}$ such that $\tilde{f} = \varphi \cdot f$ and $\tilde{\Omega} = \varphi(\Omega)$.

137 The methods we use to construct the invariants, particularly the moving frames, produces
 138 invariants that, when considered alone, are singular at points (such as critical points). How-
 139 ever, in all groups considered the invariants are rational functions of the derivatives of the
 140 function. Moreover, the denominators of these functions are powers of each other, and so it
 141 is possible to clear them by a projection technique that will be introduced in Section 3.1.

142 For the case of two-dimensional greyscale images it is often convenient to work in co-
 143 ordinates. In this case the transformation group action by a coordinate transformation
 144 $\varphi: \mathbb{R}^2 \rightarrow \mathbb{R}^2$ is given by (where f and \mathbf{x} denote the original image and coordinates, and

145 \bar{f} and $\bar{\mathbf{x}}$ the transformed versions):

146 (2.1)
$$\mathbf{x} \mapsto \bar{\mathbf{x}} = \varphi(\mathbf{x}).$$

147 The transformed image is then defined to be:

148 (2.2)
$$\bar{f}(\bar{\mathbf{x}}) = (f \circ \varphi^{-1})(\bar{\mathbf{x}}) = f(\mathbf{x}).$$

149 Derivatives of \bar{f} and f can be related by the chain rule, for example the first order deriv-
150 atives are given by:

151 (2.3)
$$\begin{aligned} f_x &= \bar{f}_{\bar{x}} \bar{x}_x + \bar{f}_{\bar{y}} \bar{y}_x \\ f_y &= \bar{f}_{\bar{x}} \bar{x}_y + \bar{f}_{\bar{y}} \bar{y}_y \end{aligned}$$

152 where $\bar{x}_x = \frac{\partial \varphi_1}{\partial x}(x, y)$, et cetera.

153 **2.2. Test image.** For each signature set that we derive, it is informative to see an example
154 signature of the kind of surface that is defined, normally a two-dimensional surface in three-
155 dimensions. We will apply a small random transformation from the relevant group to a single
156 continuous image and plot the signature before and after this transformation has been applied.
157 This is an aid to understanding rather than any form of demonstration of the robustness of
158 our signature sets.

159 The image we use is a continuous function (thus avoiding numerical issues in the approx-
160 imation of derivatives) defined on $[-1, 1] \times [-1, 1]$ as:

161 (2.4)
$$f(x, y) = \exp(-2x^2 - 4 \sin^2(y + 0.5x^2))$$

162 The function is depicted as a greyscale image in Fig. 2. We will use this function through-
163 out, using the grid on the right of the figure to help visualise both the transformation and
164 how the image is mapped into the three-dimensional signature surface.

165 **2.3. Getting Started: Translations.** The most basic transformation group of a image is
166 the translation group $T(2): \mathbb{R}^2 \rightarrow \mathbb{R}^2$ with elements of the form $\varphi(\mathbf{x}) = \mathbf{x} + \mathbf{t}$ for fixed \mathbf{t} .
167 These could arise from actions such as cropping a photo.

168 We could explicitly write the calculation in Eq. 2.3 for this case, but instead provide an
169 intuitive explanation. Consider a point in the original image, and the corresponding point in
170 the transformed one. Clearly, the intensity value of the points match, and so do their first
171 spatial derivatives. These three quantities can be used as coordinates in a new space, where
172 the two image points will correspond. Computing these coordinates for all image points will
173 define a surface in the new three-dimensional space, and the two images will produce the same
174 surface, the signature, $\mathcal{I}(f)(x, y) = (I_1, I_2, I_3)$ where $I_1 = f$, $I_2 = f_x$, $I_3 = f_y$.

175 Fig. 3 shows (a) the original image, (b) the translated image under the transformation
176 $(x, y) \mapsto (x + 0.1, y - 0.2)$, (c) the signature of one of them, (d) the superimposed pair of
177 signatures. The yellow lines in (c) correspond to places where the yellow grid from (a) has
178 been mapped to on the signature surface. The parts of the surface where the mesh gets close

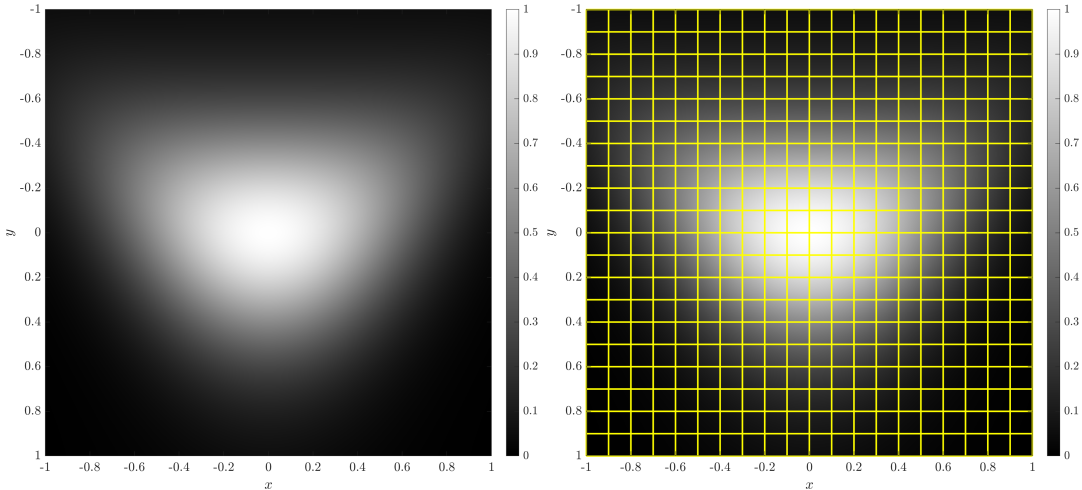


Figure 2. The test function used as an image, defined in Eq. (2.4). On the left the image itself is shown, while on the right a version with a regular grid superimposed is given.

179 together are where the function and its derivatives are tending towards zero. This occurs
 180 around the boundary of our test image and so all of these points are close together in the
 181 signature space. In (d), notice that as some of the image has moved out of frame, there are
 182 parts of the signature surfaces of the two images that do not overlap.

183 **2.4. Relevant Literature.** The theory of invariants has a rich mathematical history, start-
 184 ing from invariants of forms [Cayley, 1845], where the invariants are polynomials in the coeffi-
 185 cients of the forms, see e.g., Olver [1999], Kraft and Procesi [2002] for an overview. Geometric
 186 considerations and differential invariants followed fairly quickly [Veblen, 1929, Tresse, 1984,
 187 Bouton, 1898, Patterson, 1928], particularly because they enabled the classification of differ-
 188 ential equations into equivalence classes [Lie, 1884, Littlewood, 1944, Cartan, 1952]. More
 189 recently, this has been extended, primarily by Olver and collaborators, see e.g., Olver [1999]
 190 and Olver [1995] for summaries.

191 There has been a long-standing interest in constructing invariants for image recognition
 192 and pattern analysis, see e.g., Mundy and Zisserman [1992] and Wood [1996]. This was set
 193 in the context of Lie's invariants by Van Gool et al. [1995], where the concept of a joint (or
 194 semi-) differential invariant (an invariant that acts on the joint action of the transformation
 195 group, see Fels and Olver [1997], Olver [2001]) was introduced [Van Gool et al., 1992]; see
 196 also Hubert [2009].

197 A variety of function spaces have allowed for the creation of different sets of invariants for
 198 particular groups. For the Euclidean group, the Fourier transform provides a useful tool [Ghor-
 199 bel, 1994, Turski, 2006, Smach et al., 2007, Gauthier et al., 2008], and this can be extended
 200 to the affine group using the Fourier-Mellin transform [Reddy and Chatterji, 1996, Zhang and
 201 Williams, 2019] and the bispectrum [Kakarala, 2012, Negrinho and Aguiar, 2013]. Alterna-
 202 tively, integral invariants [Manay et al., 2006, Feng et al., 2010] and geometric moments can be
 203 computed. For the similarity group applied to images the original reference is Hu [1962], but
 204 see also Hickman [2011] for affine transformations, Flusser et al. [2009] for an implicit repre-

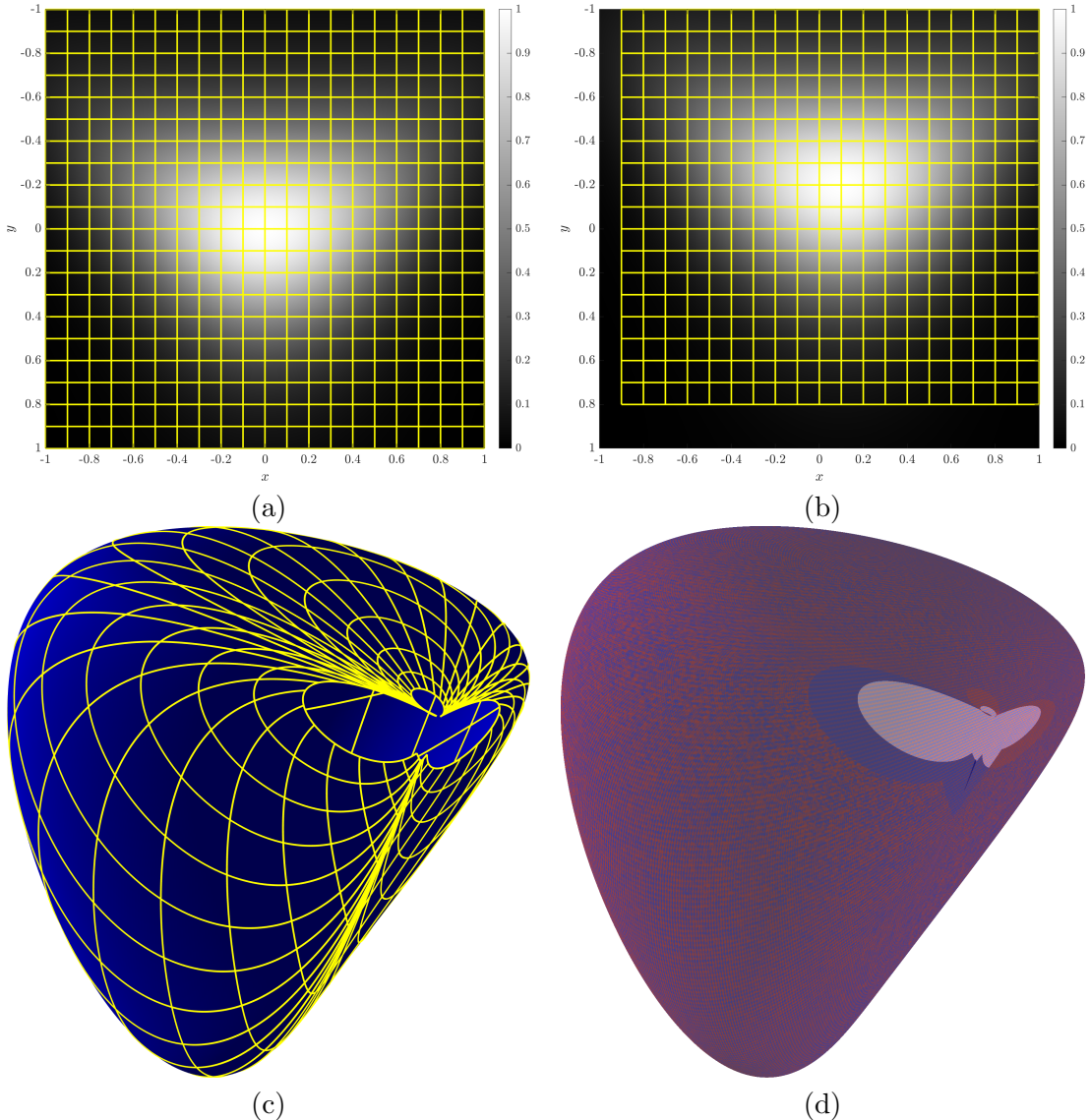


Figure 3. (a), (b) The image before and after the $T(2)$ transformation $(x, y) \mapsto (x + 0.1, y - 0.2)$. (c) the signature of the image (before translation). (d) the signatures before and after the translation superimposed.

205 sentation, and Papakostas et al. [2013] for their use in a binary pattern for image recognition,
206 which is somewhat related to the invariant features such as SURF [Bay et al., 2008].

207 The group that has been of particular interest for image analysis is the projective group,
208 because of its ubiquity in camera models. Invariants for this group have been computing using
209 points [Gros and Quan, 1992, Suk and Flusser, 2000], geometric moments [Suk and Flusser,
210 2004], curvature [Hann and Hickman, 2002], and differential and joint invariants [Hubert and
211 Olver, 2007, Arora et al., 2009, Kogan and Olver, 2015, Li et al., 2019].

212 Although there are computational challenges regarding the numerical approximation of

derivatives on images, the fact that differential invariants are robust to occlusion, cheap to compute, and well-behaved with respect to small changes in the image, has made them popular for researchers in image analysis [Florack et al., 1993]. Two particular tools have been key to this: Cartan's moving frame [Cartan, 1935] (see Section 5), and which was used to construct image invariants as early as 1994 by Faugeras [1994], and the concept of an image signature built from a set of invariants [Calabi et al., 1998]. An algorithm to compute differential and joint invariants and determine complete signature sets is described by Olver [2005, 2007]. The entire set of invariants is computed using the method of moving frames and then the signature set of a maximal set of functionally independent invariants is identified. A third step is possible, in which the dimension of the signature set is reduced by eliminating those invariants whose values can be computed from the values of derivatives of some subset of the invariants.

3. Differential invariants through tensor contraction. While we avoid the use of tensors in most of this study, there is a notable exception to be made for the Euclidean transformation group $E(2)$. In this setting we can restrict ourselves to *Cartesian tensors*, where we need make no distinction between covariance and contravariance as they are equivalent. We therefore use subscript indices exclusively.

In this setting, a Euclidean transformation acting on \mathbb{R}^2 is given by an expression of the form:

$$\bar{x}_i = a_{ij}x_j + b_j,$$

using the Einstein summation convention. The orthogonality condition is that $a_{ik}a_{jk} = a_{ki}a_{kj} = \delta_{ij}$. A Euclidean transformation $\varphi: \mathbb{R}^2 \rightarrow \mathbb{R}^2$ can also be written in matrix form as $\bar{\mathbf{x}} = \varphi(\mathbf{x}) = U\mathbf{x} + \mathbf{t}$ where the matrix U satisfies $U^T U = I$ and $\mathbf{t} \in \mathbb{R}^2$.

With respect to \mathbb{R}^2 , a Cartesian tensor of rank p , or p -tensor is a 2^p -tuple of real numbers $C_{i_1 \dots i_p}$ whose components transform under a Euclidean transformation as:

$$\bar{C}_{i_1 \dots i_p} = a_{i_1 j_1} \cdots a_{i_p j_p} C_{j_1 \dots j_p}$$

and a 0-tensor is a scalar, or invariant.

The main observation is that in this setting, the n^{th} order partial derivative operator $\partial^n / \partial x_{i_1} \cdots \partial x_{i_n}$ formally transforms as an n -tensor, [Florack et al., 1993]. Because the product of a p -tensor and a q -tensor gives a $(p+q)$ -tensor and contraction of a p -tensor yields a $(p-2)$ -tensor, a complete contraction of a tensor of even rank formed as a product of terms of the form $\partial^p f / \partial x_{i_1} \cdots \partial x_{i_p}$ will give a Euclidean invariant.

For example, up to second derivatives, we have the following Euclidean invariants, expressed as tensor contractions:

$$\begin{aligned} I_0 &= f = f \\ I_1 &= f_i f_i = f_x^2 + f_y^2 \\ I_2 &= f_{ii} = f_{xx} + f_{yy} \\ I_3 &= f_{ij} f_{ij} = f_{xx}^2 + 2f_{xy}^2 + f_{yy}^2 \\ I_4 &= f_i f_j f_{ij} = f_x^2 f_{xx} + 2f_x f_y f_{xy} + f_y^2 f_{yy}. \end{aligned} \tag{3.1}$$

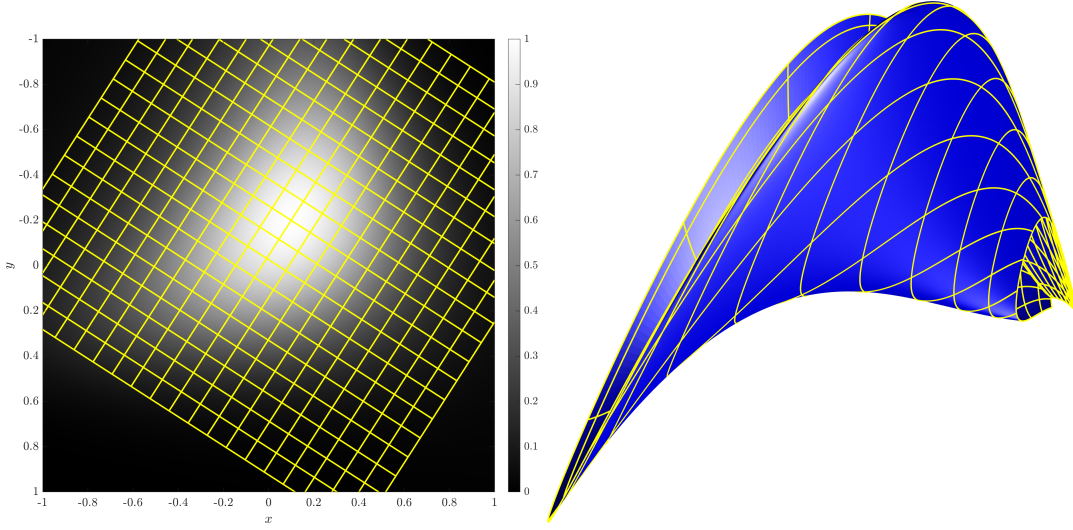


Figure 4. A sample $E(2)$ Transform and 3D signature.

248 While we can construct any number of invariants this way, there is no guarantee of func-
 249 tional independence between them. We will address this issue in Section 5 when we construct
 250 invariants of $E(2)$ and other groups using the method of moving frames. We can form a
 251 signature from any three of the invariants in Eq. (3.1), for simplicity we choose our signature
 252 to be:

253 (3.2)
$$\mathcal{I}_{E(2)} = (I_0, I_1, I_2).$$

254 A sample $E(2)$ transformation is depicted in Fig. 4 with its corresponding signature. We will
 255 defer discussion of the Special Euclidean group (which excludes reflections) until Section 5.1,
 256 where suitable invariants naturally arise from the method of moving frames.

257 **3.1. The similarity group.** The similarity group $\text{Sim}(2)$ consists of transformations of the
 258 form $\bar{\mathbf{x}} = \varphi(\mathbf{x}) = sU\mathbf{x} + \mathbf{t}$, where $U^T U = I$ and $s \in \mathbb{R} \setminus \{0\}$. It is like the Euclidean group
 259 except it also allows for isotropic scaling. In image applications, similarity transformations
 260 arise from operations like zooming.

261 Under similarity transformations, the Euclidean invariants become *relative invariants*, i.e.,
 262 each derivative introduces a multiple of s to each invariant. For example, $\bar{f}_x^2 + \bar{f}_y^2 = s^2(f_x^2 + f_y^2)$
 263 and $\bar{f}_{xx}^2 + 2\bar{f}_{xy}^2 + \bar{f}_{yy}^2 = s^4(f_{xx}^2 + 2f_{xy}^2 + f_{yy}^2)$. We refer to the power of s as the weight of the
 264 transformation. The concept of a relative invariant will be important in the rest of this paper.
 265 It follows the definition given here, except that the function weighting the invariant is more
 266 general, see Fels and Olver [1997] for more details. In contrast to that paper, we will continue
 267 to use the term weight to represent the power to which the function is raised.

268 One way to produce similarity invariants would be to take ratios of powers of the Euclidean
 269 invariants (3.1) so that the multiples of s cancel. For example $\frac{f_x^2 + f_y^2}{f_{xx}^2 + f_{yy}^2}$ is the ratio of two weight-
 270 2 relative invariants and is hence a similarity invariant. However, this invariant is singular
 271 whenever $f_{xx} + f_{yy} = 0$, which is a codimension 0 phenomenon for images.

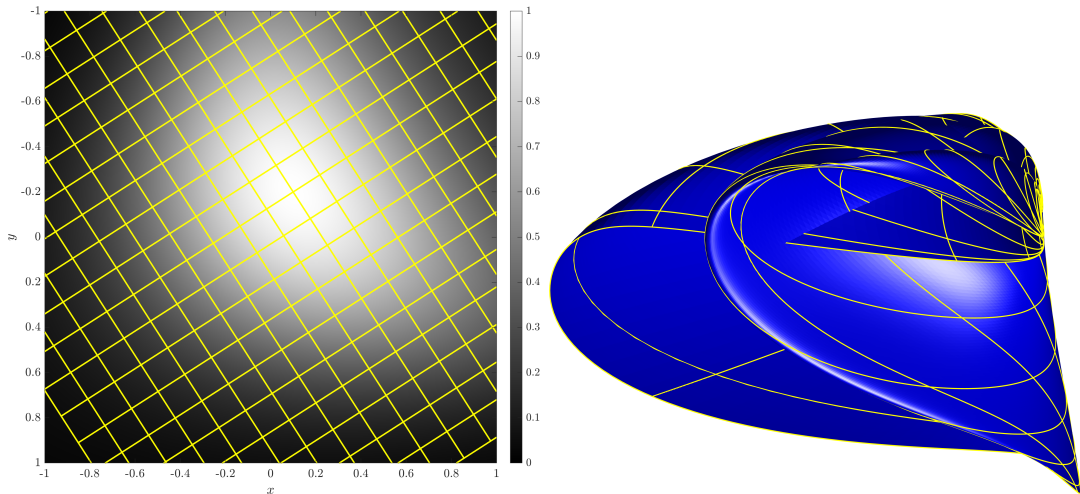


Figure 5. A sample $\text{Sim}(2)$ Transform and 3D signature.

272 A better approach is to take three invariants of the same weight. Taking I_1^2 , I_2^2 , and I_3^2
 273 from (3.1), all of which are weight 4, they can be projected on to the unit sphere, which can
 274 be multiplied by $I_0 = f$ to form a signature surface. This signature is defined by:

$$275 \quad (3.3) \quad \mathcal{I}_{\text{Sim}(2)}(f) = \frac{f}{\sqrt{I_1^4 + I_2^4 + I_3^2}}(I_1^2, I_2^2, I_3).$$

This signature is only singular when $f_x = f_y = f_{xx} = f_{yy} = f_{xy} = 0$. A sample similarity transformation and computed signature is shown in Fig. 5.

4. Differential invariants through transvectants. Another way to compute invariants is to compare the simultaneous action of a group element on separate copies of the underlying space (for planar images, \mathbb{R}^2). By identifying these spaces with each other it is possible to construct a function known as a transvectant that is a relative invariant to that group action.

We will demonstrate this for the affine group $A(2)$ and its subgroup $SA(2)$ where, following the treatment by Olver [1999], this leads to Cayley's Omega Process [Cayley, 1846].

Consider $\mathbf{x}_i \in \mathbb{R}^2, i = 1, 2$, so that \mathbf{x}_i can be written in coordinates as (x_i, y_i) ; a pair of such \mathbf{x} lie in $\mathbb{R}^2 \times \mathbb{R}^2$. Now consider applying the same affine transformation to each \mathbf{x} independently: $\mathbf{x}_i \mapsto A\mathbf{x}_i + \mathbf{b}$ where $A \in GL(2, \mathbb{R})$ and $\mathbf{b} \in \mathbb{R}^2$. Then the Omega Process is a second-order differential operator defined by:

$$288 \quad (4.1) \qquad \Omega_{ij} = \begin{vmatrix} \frac{\partial}{\partial x_i} & \frac{\partial}{\partial y_i} \\ \frac{\partial}{\partial x_j} & \frac{\partial}{\partial y_j} \end{vmatrix} = \frac{\partial^2}{\partial x_i \partial y_j} - \frac{\partial^2}{\partial x_j \partial y_i}.$$

Under the above affine transformation, $\Omega_{ij} \mapsto (\det A)^{-1}\Omega_{ij}$, and is therefore a relative invariant. Note that $(\det A)^{-1}$ has no dependence on the coordinates. The Omega Process can be applied to products of pairs of smooth functions as follows, writing $\frac{\partial f}{\partial x}$ as f_x :

$$292 \quad (4.2) \quad \Omega_{ij}(f(x_i, y_i)g(x_j, y_j)) = f_{x_i}g_{y_i} - f_{y_i}g_{x_i}.$$

293 Identifying $x_i = x_j = x, y_i = y_j = y$ gives functions of x and y that only vary by a scaling
 294 factor of $(\det A)^{-1}$ when \mathbf{x} is mapped by an affine transformation. This matches the definition
 295 of a first-order partial transvectant of two functions:

296 (4.3) $\text{tr} \Omega_{ij} f(x_i, y_i) g(x_j, y_j),$

297 where tr is the operator that identifies the coordinates of each function $x_i = x_j = x, y_i = y_j =$
 298 y .

299 This can be generalised to n functions $f^{(1)}(x_1, y_1), \dots, f^{(n)}(x_n, y_n)$ and r -th order [Olver,
 300 1995] to define a partial transvectant as:

301 (4.4) $\text{tr} \left[(\prod_{k=1}^r \Omega_{i_k j_k}) f^{(1)}(x_1, y_1) f^{(2)}(x_2, y_2), \dots f^{(n)}(x_n, y_n) \right],$

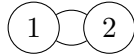
302 where $i_k \neq j_k \in \{1, \dots, n\}$.

303 Under this formula there is a factor $(\det A)^{-r}$ in place of $(\det A)^{-1}$ that we saw previously,
 304 when all n copies of \mathbb{R}^2 are transformed by the same affine function $\mathbf{x} \mapsto A\mathbf{x} + \mathbf{b}$. Note that
 305 the individual pairwise Omega processes commute.

306 For the current case it is sufficient to consider n copies of the same function f . If we
 307 represent each copy of \mathbb{R}^2 as a node in an undirected graph, and each Omega process Ω_{ij}
 308 as an edge joining nodes i and j , a partial transvectant can be compactly represented in a
 309 graphical form. For example, consider a weight 2 transvectant defined as:

$$\begin{aligned} 310 \quad & \text{tr} [(\Omega_{12} \Omega_{12}) f(x_1, y_1) f(x_2, y_2)] \\ 311 \quad & = \text{tr} [(\partial_{x_1 y_2} - \partial_{x_2 y_1})(\partial_{x_1 y_2} - \partial_{x_2 y_1}) f(x_1, y_1) f(x_2, y_2)] \\ 312 \quad & = \text{tr} [(\partial_{x_1 y_2} - \partial_{x_2 y_1})(f_x(x_1, y_1) f_y(x_2, y_2) - f_y(x_1, y_1) f_x(x_2, y_2))] \\ 313 \quad & = \text{tr} [f_{xx}(x_1, y_1) f_{yy}(x_2, y_2) - f_{xy}(x_1, y_1) f_{xy}(x_2, y_2)] \\ 314 \quad & = 2f_{xx}(x, y) f_{yy}(x, y) - 2f_{xy}(x, y)^2. \end{aligned}$$

316 This is a degree 2 partial transvectant as it involves derivatives of f up to second-order, and
 317 can be represented graphically by the following diagram:



319 where the double edge corresponds to the two copies of Ω_{12} (the names are purely for convenience), i.e., the weight is the number of edges in the graph.

321 Tables 1 and 2 shows all possible non-zero partial transvectants of A_2 up to weight 4 that
 322 can be generated in this way.

323 Owing to the group-subgroup structure some of these partial transvectants appear in
 324 signatures from other transformation groups, so for future reference, we define:

$$\begin{aligned} 325 \quad & C = f_{xx} f_{yy} - f_{xy}^2, \\ & D = f_x^2 f_{yy} - 2f_x f_y f_{xy} + f_{xx} f_y^2, \\ & E = f_{xxx} f_y^3 - 3f_{xxy} f_x f_y^2 + 3f_{xyy} f_x^2 f_y - f_{yyy} f_x^3. \end{aligned}$$

Degree	Weight	Diagram	Partial transvectant
2	2		$2f_{xx}f_{yy} - 2(f_{xy})^2$
2	2		$(f_x)^2 f_{yy} - 2f_x f_y f_{xy} + f_{xx} (f_y)^2$
2	4		$2(f_{xx})^2 (f_{yy})^2 - 4f_{xx}f_{yy}(f_{xy})^2 + 2(f_{xy})^4$
2	4		$(f_x)^2 f_{xx} (f_{yy})^2 - (f_x)^2 f_{yy} (f_{xy})^2 - 2f_x f_{xx} f_y f_{yy} f_{xy} + 2f_x f_y (f_{xy})^3 + (f_{xx})^2 (f_y)^2 f_{yy} - f_{xx} (f_y)^2 (f_{xy})^2$
3	3		$-f_x f_{xx} f_{yyy} - f_x f_{yy} f_{xxy} + 2f_x f_{xy} f_{xyy} + f_{xx} f_y f_{xyy} + f_{xxx} f_y f_{yy} - 2f_y f_{xy} f_{xxy}$
3	3		$-(f_x)^3 f_{yyy} + 3(f_x)^2 f_y f_{xyy} - 3f_x (f_y)^2 f_{xxy} + f_{xxx} (f_y)^3$
3	4		$2f_{xx}f_{yyy}f_{xxy} - 2f_{xx}(f_{xy})^2 + 2f_{xxx}f_y f_{yy} f_{xxy} - 2f_{xxx}f_{yyy}f_{xy} - 2f_{yy}(f_{xy})^2 + 2f_{xy}f_{xyy}f_{xxy}$
3	4		$-f_x f_{xx} f_{yy} f_{xy} + f_x f_{xx} f_{yyy} f_{xy} - f_x f_{xxx} (f_{yy})^2 + 3f_x f_{yy} f_{xy} f_{xxy} - 2f_x (f_{xy})^2 f_{xyy} - (f_{xx})^2 f_y f_{yyy} - f_{xx} f_y f_{yy} f_{xxy} + 3f_{xx} f_y f_{xy} f_{xyy} + f_{xxx} f_y f_{yy} f_{xy} - 2f_y (f_{xy})^2 f_{xxy}$
3	4		$2(f_x)^2 f_{yyy} f_{xxy} - 2(f_x)^2 (f_{xy})^2 - 2f_x f_{xxx} f_y f_{yyy} + 2f_x f_y f_{xy} f_{xxy} + 2f_{xxx} (f_y)^2 f_{xyy} - 2(f_y)^2 (f_{xy})^2$
3	4		$-(f_x)^3 f_{yy} f_{xxy} + (f_x)^3 f_{yyy} f_{xy} - (f_x)^2 f_{xx} f_y f_{yyy} + 2(f_x)^2 f_y f_{yy} f_{xxy} - (f_x)^2 f_y f_{xy} f_{xyy} + 2f_x f_{xx} (f_y)^2 f_{xyy} - f_x f_{xxx} (f_y)^2 f_{yy} - f_x (f_y)^2 f_{xy} f_{xxy} - f_{xx} (f_y)^3 f_{xxy} + f_{xxx} (f_y)^3 f_{xy}$

Table 1

Details and graphical representations of all partial transvectants up to degree 3 of copies of a function f under a transformation in $A(2)$.

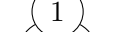
Degree	Weight	Diagram	Partial transvectant
4	4		$f_{xxxx}f_{yyyy} - 4f_{xyyy}f_{xxxy} + 3f_{xxyy}^2$
4	4		$f_{xx}^2 f_{yyyy} + 2f_{xx} f_{yy} f_{xxyy} - 4f_{xx} f_{xy} f_{xyyy} - 4f_{yy} f_{xy} f_{xxxy} + 4f_{xy}^2 f_{xxyy} + f_{xxxx} f_{yy}^2$
4	4		$f_x f_{xxx} f_{yyyy} - f_x f_{yyy} f_{xxxy} + 3f_x f_{xyy} f_{xxyy} - 3f_x f_{xyy} f_{xxyy} f_{xxy} - f_{xxx} f_y f_{xyyy} + f_{xxxx} f_y f_{yyy} - 3f_y f_{xyy} f_{xxxy} + 3f_y f_{xxy} f_{xyyy}$
4	4		$(f_x)^4 f_{yyyy} - 4(f_x)^3 f_y f_{xyyy} + 6(f_x)^2 (f_y)^2 f_{xxyy} - 4f_x (f_y)^3 f_{xxxy} + f_{xxxx} (f_y)^4$

Table 2

Details and graphical representations of all partial transvectants of weight 4 of copies of a function f under a transformation in A(2).

4.1. Signatures of $SA(2)$ and $A(2)$. The action of the affine group $A(2)$ arises in images as the motion of planar objects in images taken from a distant camera. Recall that because of the subgroup relationship, invariants of $A(2)$ are automatically invariants of $SA(2)$, but not necessarily vice versa. Any of the partial transvectants found in Tables 1 and 2 are relative invariants of $SA(2)$ (as the determinant is 1). Hence, we can form a signature for $SA(2)$ by choosing any combination of partial transvectants. We choose a signature with three components so that it can be visualised as a three-dimensional surface; note that this will not be complete and may well have a very large bad set. For example, we can choose the function value together with C and D from Eq. (4.5) to form the signature:

$$335 \quad (4.6) \qquad \qquad \qquad \mathcal{I}_{SA(2)}(f) = (f, C, D).$$

Fig. 6 shows the signature of our test image under an $SA(2)$ transformation.

For $A(2)$ the weight of the partial transvectants prevents them from being invariants. There are two options to create a signature. One is to select ratios of partial transvectants, as discussed in Section 3.1. It is then beneficial to choose the numerator and denominator so that they have different critical points, which can be achieved by adding together partial transvectants of the same weight as appropriate. Instead, we employ the same normalisation strategy as previously, projecting the weight four relative invariants (C^2, D^2, E) onto the unit hypersphere and multiplying by f . In this way, our signature is:

$$344 \quad (4.7) \quad \mathcal{I}_{A(2)} = \frac{f}{\sqrt{C^4 + D^4 + E^2}} (C^2, D^2, E)$$

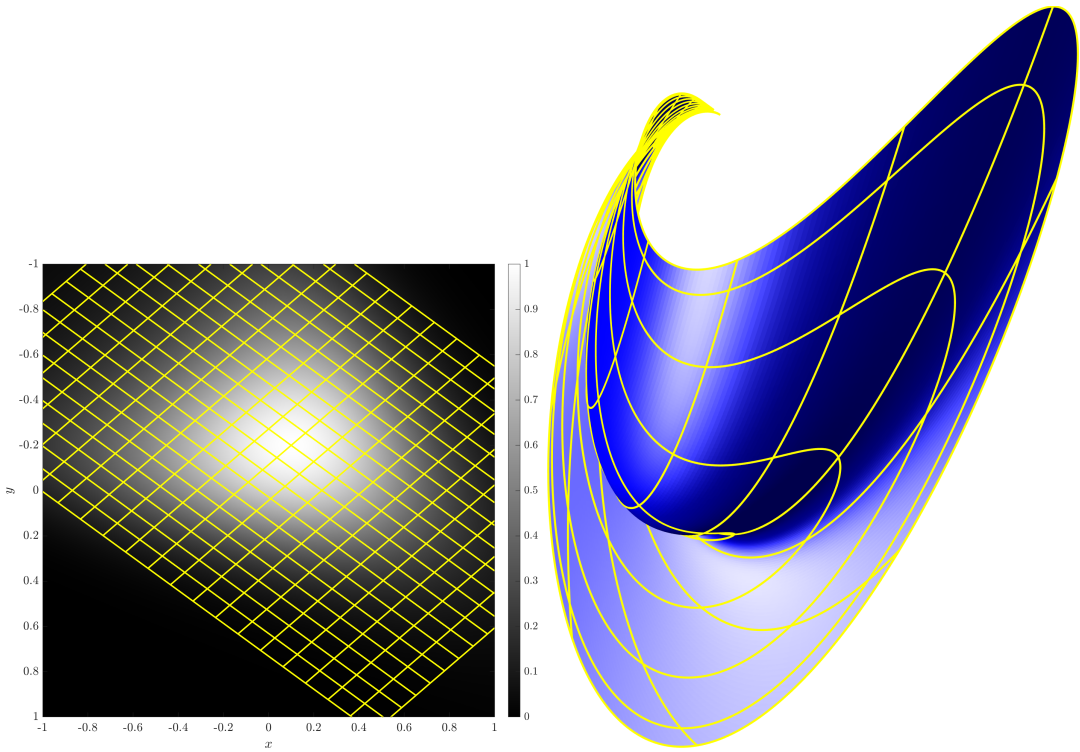


Figure 6. A sample $SA(2)$ transformation applied to our test function, and the corresponding signature.

345 We will subject our test image to the special affine transformation: Fig. 7 shows the
 346 signature of our test image under this transformation.

347 **5. Differential invariants through moving frames.** So far, the methods that we have
 348 seen to construct differential invariants for particular groups are not directly generalisable. It
 349 is natural to ask if there is an algorithmic approach that will yield invariants more directly.
 350 The answer is a qualified yes. There is a general method, based on Cartan's method of
 351 moving frames, that is generally applicable, but finding good solutions with it still requires
 352 some ingenuity in general. Olver and co-authors have popularised the approach and made
 353 it applicable to object recognition based on outline curves, see [Olver \[2005\]](#) for an overview,
 354 and note particularly the original application paper [\[Calabi et al., 1998\]](#). We introduce the
 355 method here and then demonstrate its use to find invariants to further groups, but for further
 356 technical details see [Olver \[1999\]](#).

357 A moving frame is a mapping into a group \mathcal{G} that provides a frame of reference along a
 358 manifold. It was extended by [Cartan \[1935\]](#) to the ‘method of moving frames’. If the group
 359 \mathcal{G} is a Lie group then it has a homogeneous space and a frame of reference can be applied
 360 on the manifold structure of the group. Considering the actions of such a transformation
 361 group enables the identification of invariants to that group since it defines a \mathcal{G} -equivariant
 362 mapping. A (right-) moving frame is a smooth \mathcal{G} -equivariant map $\rho : \mathcal{M} \rightarrow \mathcal{G}$ such that
 363 $\rho(g \cdot z) = \rho(z) \cdot g^{-1}$, where $z \in J^d$. It is necessary [\[Olver, 2001\]](#) for the group act freely. This

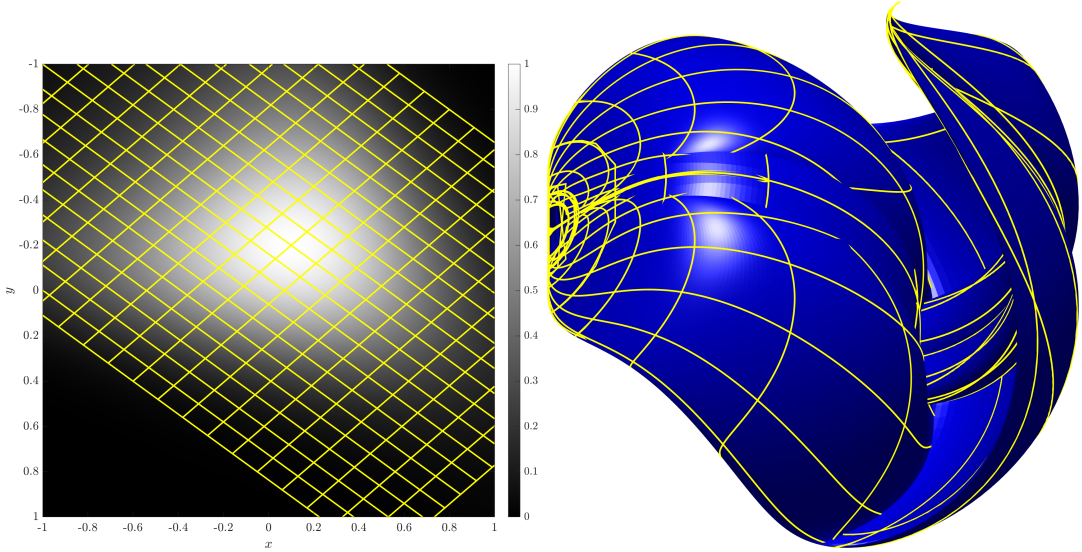


Figure 7. A sample $A(2)$ transformation applied to our test function, and the corresponding signature.

means that the group action needs to be extended to the entire jet space of derivatives up to order d by implicit differentiation of the group action, a process known as prolongation.

The procedure to construct differential invariants to the action of Lie group \mathcal{G} acting on manifold \mathcal{M} using the method of moving frames is as follows:

1. Prolong the group action to the jet space of d -th order derivatives: $F : J^d \rightarrow \mathbb{R}$.
2. Apply Cartan normalisation:
 - (a) Choose a local cross-section to the group orbits, i.e., a $(d - \dim \mathcal{G})$ -dimensional submanifold \mathcal{K} that intersects transversally at most once with each orbit
 - (b) \mathcal{K} is specified by $\dim \mathcal{G}$ independent equations $Z_i(z) = c_i$, for $z \in J^d$, and Z_i scalar-valued functions and c_i constants.
 - (c) The right-moving frame $g = \rho(z)$ is found by solving the normalisation questions $Z_i(g \cdot z) = c_i$ for the group parameters g (in terms of z). In other words, the moving frame is the transformation back to the cross-section.
3. The differential invariants are not affected by the action of the group: $I(g \cdot z) = I(z) \forall z \in \text{dom}I$, or equivalently, if it is constant on the orbits.
4. Hence F is made invariant by transforming it with a group action: $I(z) = F(g \cdot z)|_{g=\rho(z)}$.

Cartan normalisation can be considered as identifying a canonical subspace (with some coordinates fixed) in the jet space to which any point in the jet space can be mapped by a group action.

Olver [1999] uses the group $SE(2)$ on curves as an example, recovering the Euclidean curvature as a second-order invariant. We continue this example to compute invariants to $SE(2)$ for images, before moving on to other planar Lie group examples: $E(2)$, the Möbius group ($PSL(2, \mathbb{C})$) and the projective group ($PSL(3, \mathbb{R})$). Finally, we apply the method to an infinite-dimensional pseudo-Lie group, the conformal diffeomorphisms.

389 **5.1. The Special Euclidean Group SE(2).** An element of the special Euclidean group
 390 $SE(2)$ acts on an element (x, y) of \mathbb{R}^2 to produce (\bar{x}, \bar{y}) as:

391
$$\begin{aligned}\bar{x} &= x \cos \theta - y \sin \theta + t_x \\ \bar{y} &= x \sin \theta + y \cos \theta + t_y.\end{aligned}$$

392 We prolong the group action to form the jet space J^2 with coordinates $(x, y, f, f_x, f_y, f_{xx}, f_{xy}, f_{yy})$ █
 393 via the chain rule. The transformation rule for the derivatives is given by:

394 (5.1)
$$\begin{bmatrix} \bar{f}_{\bar{x}} \\ \bar{f}_{\bar{y}} \\ \bar{f}_{\bar{x}\bar{x}} \\ \bar{f}_{\bar{x}\bar{y}} \\ \bar{f}_{\bar{y}\bar{y}} \end{bmatrix} = \begin{bmatrix} c & -s & 0 & 0 & 0 \\ s & c & 0 & 0 & 0 \\ 0 & 0 & c^2 & -2cs & s^2 \\ 0 & 0 & cs & c^2 - s^2 & -cs \\ 0 & 0 & s^2 & 2cs & c^2 \end{bmatrix} \begin{bmatrix} f_x \\ f_y \\ f_{xx} \\ f_{xy} \\ f_{yy} \end{bmatrix},$$

395 where $c = \cos \theta$ and $s = \sin \theta$. Because the group has three parameters, we choose the cross-
 396 section of the group orbits to be $\bar{x} = 0, \bar{y} = 0, \bar{f}_y = 0$. We also require that $\bar{f}_{\bar{x}} > 0$ to uniquely
 397 define the moving frame. Note that the group action is locally free (away from critical points)
 398 when prolonged to J^1 , however we prolong to J^2 in order to compute invariants. The moving
 399 frame is then given by the prolonged Euclidean transformation that maps an element of J^2
 400 to this cross-section. It can be thought of as rotating the image about that point so that its
 401 gradient is pointing in the positive x direction, and then translating the image so the point is
 402 mapped to the origin.

403 This choice of moving frame gives $\cos \theta = f_x / \|\nabla f\|$ and $\sin \theta = -f_y / \|\nabla f\|$. The param-
 404 eters t_x, t_y are then $t_x = -x \cos \theta + y \sin \theta$ and $t_y = -x \sin \theta - y \cos \theta$, however these have no
 405 effect on the derivatives, and will henceforth be ignored.

406 The remaining elements not fixed by the cross-section, \bar{f} , $\bar{f}_{\bar{x}}$, $\bar{f}_{\bar{x}\bar{x}}$, $\bar{f}_{\bar{x}\bar{y}}$, and $\bar{f}_{\bar{y}\bar{y}}$, are therefore
 407 all invariant. This gives the following set of invariants:

408 (5.2)
$$\begin{aligned}K_0 &= f \\ K_1 &= f_x^2 + f_y^2 && (= \bar{f}_{\bar{x}}^2) \\ K_2 &= f_x^2 f_{xx} + 2f_x f_y f_{xy} + f_y^2 f_{yy} && (= K_1 \bar{f}_{\bar{x}\bar{x}}) \\ K_3 &= f_x f_y (f_{yy} - f_{xx}) + f_{xy} (f_x^2 - f_y^2) && (= K_1 \bar{f}_{\bar{x}\bar{y}}) \\ K_4 &= f_y^2 f_{xx} - 2f_x f_y f_{xy} + f_x^2 f_{yy} && (= K_1 \bar{f}_{\bar{y}\bar{y}}).\end{aligned}$$

409 Note that we have multiplied each of the second derivative invariants by the invariant K_1 so
 410 that they decay smoothly to zero at critical points. Interestingly, K_4 is the affine invariant D
 411 from Eq. (4.5) and K_1 and K_2 are also Euclidean invariants, so we need to include K_3 in our
 412 signature:

413 (5.3)
$$I_{SE(2)}(f) = (f, K_1, K_3).$$

414 Fig. 8 shows the signature of our test image under a sample transformation of $SE(2)$.

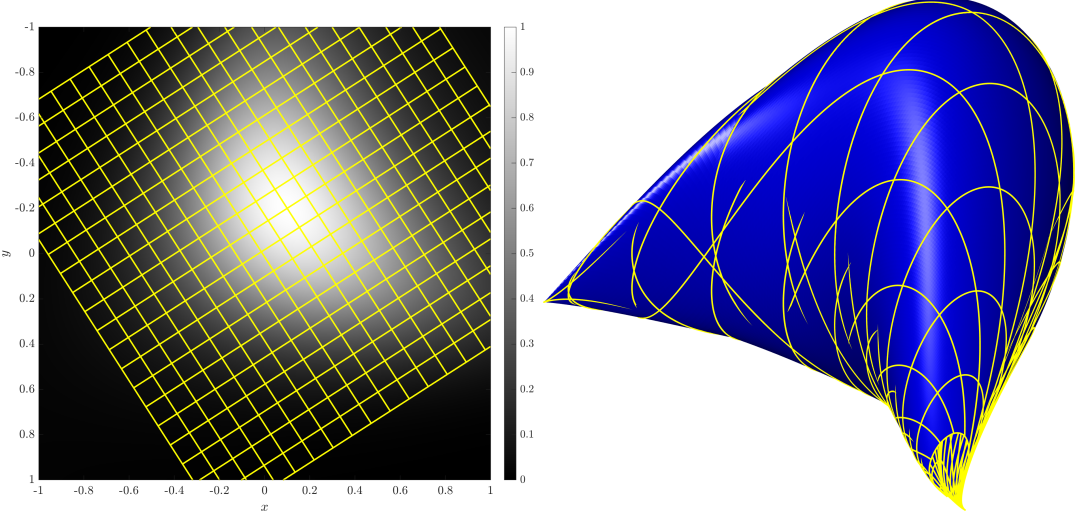


Figure 8. A sample $SE(2)$ transform and 3D signature.

415 **5.2. The Euclidean Group $E(2)$.** An element of the Euclidean group $E(2)$ maps an ele-
416 ment (x, y) of \mathbb{R}^2 to (\bar{x}, \bar{y}) as:

417

$$\begin{aligned}\bar{x} &= x\varepsilon \cos \theta - y\varepsilon \sin \theta + t_x \\ \bar{y} &= x \sin \theta + y \cos \theta + t_y.\end{aligned}$$

418 where $\varepsilon \in \{-1, 1\}$ and the remaining parameters are the same as for $SE(2)$. If $\varepsilon = 1$ it is a
419 rigid transformation, and if $\varepsilon = -1$ it contains a reflection.

420 This time, the group action is not free on J^1 (with elements of the form (x, y, f, f_x, f_y))
421 away from critical points because there are two possible transformations that map to the
422 cross-section $(0, 0, \bar{f}, \bar{f}_{\bar{x}}, 0)$ where $\bar{f}_{\bar{x}} > 0$, one that reflects the gradient into the positive x
423 direction, and one that rotates.

424 We again prolong the group action to J^2 , but this time we expect to need to use a second
425 derivative term to determine ε for the moving frame. The derivative transformations are given
426 by:

427 (5.4)

$$\begin{bmatrix} \bar{f}_{\bar{x}} \\ \bar{f}_{\bar{y}} \\ \bar{f}_{\bar{x}\bar{x}} \\ \bar{f}_{\bar{x}\bar{y}} \\ \bar{f}_{\bar{y}\bar{y}} \end{bmatrix} = \begin{bmatrix} \varepsilon c & -\varepsilon s & 0 & 0 & 0 \\ s & c & 0 & 0 & 0 \\ 0 & 0 & c^2 & -2cs & s^2 \\ 0 & 0 & \varepsilon cs & \varepsilon(c^2 - s^2) & -\varepsilon cs \\ 0 & 0 & s^2 & 2cs & c^2 \end{bmatrix} \begin{bmatrix} f_x \\ f_y \\ f_{xx} \\ f_{xy} \\ f_{yy} \end{bmatrix},$$

428 where again $c = \cos \theta$ and $s = \sin \theta$.

429 We begin by choosing the same cross-section as for $SE(2)$, namely $\bar{x} = 0, \bar{y} = 0, \bar{f}_{\bar{y}} =$
430 $0, \bar{f}_{\bar{x}} > 0$. This gives $\cos \theta = \varepsilon f_x / \|\nabla f\|$ and $\sin \theta = -\varepsilon f_y / \|\nabla f\|$. Under this transformation,
431 regardless of whether $\varepsilon = 1$ or $\varepsilon = -1$, the derivative $\bar{f}_{\bar{x}} = \|\nabla f\|$. The only second derivative
432 term in which ε appears is the $\bar{f}_{\bar{x}\bar{y}}$ term, so we use this to resolve the sign. Substituting in for

433 $\cos \theta, \sin \theta$, we see that:

$$434 \quad \bar{f}_{\bar{x}\bar{y}} = \frac{\varepsilon(f_x f_y (f_{yy} - f_{xx}) + (f_x^2 - f_y^2) f_{xy})}{f_x^2 + f_y^2}.$$

435 This suggests choosing ε to make $\bar{f}_{\bar{x}\bar{y}} \geq 0$. The moving frame is then fully specified, and
436 the remaining derivatives give the same invariants K_0, K_1, K_2, K_4 as for $SE(2)$, (5.2), the one
437 difference being:

$$438 \quad (5.5) \quad \hat{K}_3 = |f_x f_y (f_{yy} - f_{xx}) + f_{xy} (f_x^2 - f_y^2)|$$

439 These invariants are a functionally independent, complete, set of polynomial differential
440 invariants up to second derivatives. Note that the invariants found previously by tensor
441 contraction Eq. (3.1) in Section 3 can be expressed in terms of them:

$$442 \quad f = f = K_0$$

$$443 \quad f_i f_i = f_x^2 + f_y^2 = K_1$$

$$444 \quad f_{ii} = f_{xx} + f_{yy} = \frac{K_2 + K_4}{K_1}$$

$$445 \quad f_{ij} f_{ij} = f_{xx}^2 + 2f_{xy}^2 + f_{yy}^2 = \frac{K_2^2 + K_4^2 + 2K_3^2}{K_1^2}$$

$$446 \quad f_i f_j f_{ij} = f_x^2 f_{xx} + 2f_x f_y f_{xy} + f_y^2 f_{yy} = K_2.$$

447 **5.3. The Möbius Group.** The Möbius group $PSL(2, \mathbb{C})$ acts on the Riemann sphere
448 $\overline{\mathbb{C}} = \mathbb{C} \cup \infty$ by:

$$450 \quad (5.6) \quad \phi: \overline{\mathbb{C}} \rightarrow \overline{\mathbb{C}}, \quad \phi(z) = \frac{\alpha z + \beta}{\gamma z + \delta}, \quad \alpha, \beta, \gamma, \delta \in \mathbb{C}, \quad \alpha\delta - \beta\gamma \neq 0.$$

451 Identifying \mathbb{R}^2 with \mathbb{C} , the Möbius group is a real 6-dimensional local Lie group acting
452 on \mathbb{R}^2 . It is the smallest nonlinear planar group that contains $SE(2)$, and it also has direct
453 applications in image processing since it arises in the *conformal camera* model of vision, in
454 which scenes are projected radially onto a sphere [Lenz, 1990, Turski, 2004]; it is also the set
455 of biholomorphic maps of the Riemann sphere.

456 We are free to take $\delta = 1$. Then $\bar{f} = f$ means that z is translated to β ; we can therefore
457 take $\beta = 0$. This leaves 4 group parameters a, b, c, d , where $\alpha = a + ib$, $\gamma = c + id$, to be
458 determined as follows. We prolong the action to second derivatives of f , which is sufficient
459 to allow the group to act freely. There are 5 derivatives of f up to order 2, so there will be
460 at least 1 invariant. In order to find further invariants the prolongation to 3rd derivatives is
461 required, which will result in at least another four invariants. This simple counting argument
462 works because the group acts freely on the prolongation.

463 The prolonged action is:

$$464 \quad (5.7) \quad \begin{bmatrix} \bar{f}_{\bar{x}} \\ \bar{f}_{\bar{y}} \\ \bar{f}_{\bar{x}\bar{x}} \\ \bar{f}_{\bar{x}\bar{y}} \\ \bar{f}_{\bar{y}\bar{y}} \end{bmatrix} = \begin{bmatrix} a & b & 0 & 0 & 0 \\ -b & a & 0 & 0 & 0 \\ 2\mu & -2\rho & a^2 & 2ab & b^2 \\ 2\rho & 2\mu & -ab & a^2 - b^2 & ab \\ -2\mu & 2\rho & b^2 & -2ab & a^2 \end{bmatrix} \begin{bmatrix} f_x \\ f_y \\ f_{xx} \\ f_{xy} \\ f_{yy} \end{bmatrix}.$$

465 where $\mu = bd - ac$ and $\rho = bc + ad$.

466 The moving frame calculation is then:

1. The frame $\bar{f}_{\bar{x}} = 1, \bar{f}_{\bar{y}} = 0$ determines two group parameters:

$$a = f_x/(f_x^2 + f_y^2), \quad b = f_y/(f_x^2 f_y^2).$$

2. The frame $\bar{f}_{\bar{x}\bar{y}} = \bar{f}_{\bar{y}\bar{y}} = 0$ determines the next group parameters:

$$c = (2f_x f_y f_{xy} - f_{xx} f_y^2 - f_{yy} f_x^2)/(2f_x^2 + f_y^2)^2$$

$$d = (f_{xy} f_x^2 - f_x f_y f_{xx} - f_{xy} f_y^2 - f_{yy} f_x f_y)/(2f_x^2 + f_y^2)^2.$$

3. The second-order invariant is then given by $\bar{f}_{\bar{x}\bar{x}}$ using Eq. (5.7):

$$\bar{f}_{\bar{x}\bar{x}} = \frac{f_{xx} + f_{yy}}{f_x^2 + f_y^2}.$$

467 The four third-order invariants can be deduced from the moving frame. They are rational
 468 functions with numerators of degree 6 and denominators $(f_x^2 + f_y^2)^4$, and are relative invariants
 469 of weight 8. Clearing denominators so as to work with polynomials, we choose $M_1 = (f_{xx} +$
 470 $f_{yy})^4$ and two of the four third-order invariants M_2 and M_3 :

$$\begin{aligned} 471 \quad M_2 &= f_y^5 f_{yyy} + \frac{9}{2} f_y^2 f_{yy} f_x^2 + f_y^3 f_{yyy} f_x^2 + \frac{3}{2} f_{yy}^2 f_x^4 - 9 f_y^3 f_{yy} f_x f_{xy} + 3 f_y f_{yy} f_x^3 f_{xy} + \frac{3}{2} f_y^4 f_{xy}^2 \\ 472 \quad &- 9 f_y^2 f_x^2 f_{xy}^2 + \frac{3}{2} f_z^4 f_{xy}^2 + 3 f_y^4 f_x f_{xyy} + 3 f_y^2 f_x^3 f_{xyy} + 3 f_y^4 f_{yy} f_{xx} + 3 f_{yy} f_x^4 f_{xx} + 3 f_y^3 f_x f_{xy} f_{xx} \\ 473 \quad &- 9 f_y f_x^3 f_{xy} f_{xx} + \frac{3}{2} f_y^4 f_{xx}^2 + \frac{9}{2} f_y^2 f_x^2 f_{xx}^2 + 3 f_y^3 f_x^2 f_{xxy} + 3 f_y f_x^4 f_{xxy} + f_y^2 f_x^3 f_{xxx} + f_x^5 f_{xxx}, \\ 474 \end{aligned}$$

$$\begin{aligned} 475 \quad M_3 &= -3 f_y f_{yy}^2 f_x^3 + f_y^2 f_{yyy} f_x^3 + f_{yyy} f_x^5 + 9 f_y^2 f_{yy} f_x^2 f_{xy} - 3 f_{yy} f_x^4 f_{xy} - 6 f_y^3 f_x f_{xy}^2 + 6 f_y f_x^3 f_{xy}^2 \\ 476 \quad &- 3 f_y^3 f_x^2 f_{xyy} - 3 f_y f_x^4 f_{xyy} - 3 f_y^3 f_{yy} f_x f_{xx} + 3 f_y f_{yy} f_x^3 f_{xx} + 3 f_y^4 f_{xy} f_{xx} - 9 f_y^2 f_x^2 f_{xy} f_{xx} \\ 477 \quad &+ 3 f_y^3 f_x f_{xx}^2 + 3 f_y^4 f_x f_{xxy} + 3 f_y^2 f_x^3 f_{xxy} - f_y^5 f_{xxx} - f_y^3 f_x^2 f_{xxx}. \\ 478 \end{aligned}$$

479 We then form a signature by our usual projection method from the image f and these three
 480 weight 8 relative invariants:

$$481 \quad (5.8) \quad \mathcal{I}_{\text{M\"obius}}(f) = \frac{f}{\sqrt{M_1^2 + M_2^2 + M_3^2}}(M_1, M_2, M_3)$$

482 An example is shown in Fig. 9, although note that the signature is singular when $f_x = f_y =$
 483 $f_{xx} + f_{yy} = 0$, a codimension 1 phenomenon for images.

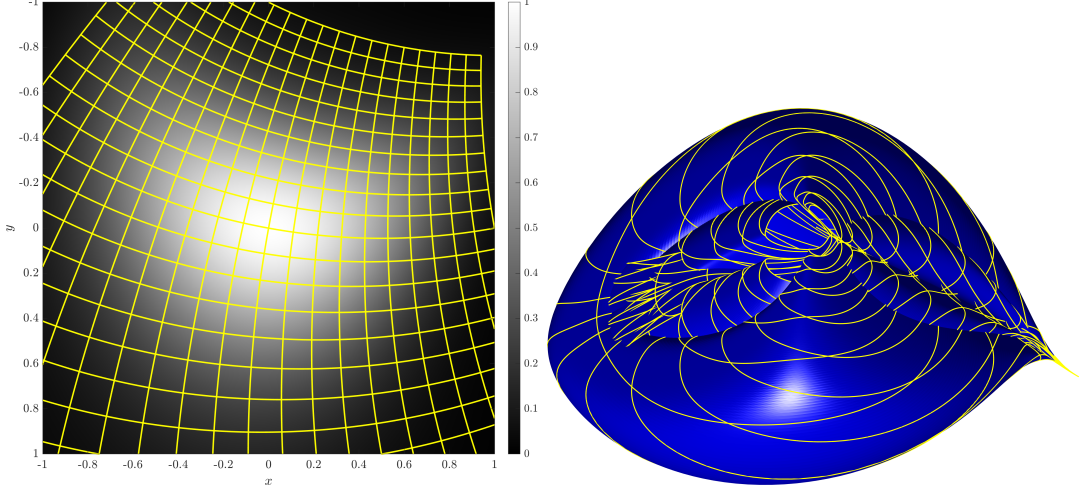


Figure 9. A sample Möbius transform and 3D signature.

484 **5.4. The Projective Group.** The action of the projective group arises naturally through
 485 the movements of the camera viewing planar objects. We consider the eight-dimensional group
 486 $PSL(3, \mathbb{R})$ acting on \mathbb{R}^2 by projective transformations, i.e.,

487 (5.9)
$$(x, y) \mapsto \left(\frac{ax + by + j}{l + gx + hy}, \frac{cx + dy + k}{l + gx + hy} \right).$$

488 Requiring that $\bar{f} = f$ enables us to clear the translation coefficients, so $j = k = 0$; for
 489 convenience we will also take $l = 1$. This leaves 6 group parameters (a, b, c, d, g, h) to be
 490 determined. For free action it is necessary to prolong the group action to 3rd derivatives of
 491 f . Since there are 9 derivatives of f of order 1, 2, and 3, there will be at least 3 invariants.
 492 The prolonged action is:

493 (5.10)
$$\begin{bmatrix} \bar{f}_{\bar{x}} \\ \bar{f}_{\bar{y}} \\ \bar{f}_{\bar{x}\bar{x}} \\ \bar{f}_{\bar{x}\bar{y}} \\ \bar{f}_{\bar{y}\bar{y}} \\ \bar{f}_{\bar{x}\bar{x}\bar{x}} \\ \bar{f}_{\bar{x}\bar{x}\bar{y}} \\ \bar{f}_{\bar{x}\bar{y}\bar{y}} \\ \bar{f}_{\bar{y}\bar{y}\bar{y}} \end{bmatrix} = \begin{bmatrix} a & c & 0 & 0 & 0 & 0 & 0 & 0 \\ b & d & 0 & 0 & 0 & 0 & 0 & 0 \\ -2ag & -2cg & a^2 & 2ac & c^2 & 0 & 0 & 0 \\ -bg - ah - dg - ch & ab & bc + ad & cd & 0 & 0 & 0 & 0 \\ -2bh & -2dh & b^2 & 2bd & d^2 & 0 & 0 & 0 \\ 6ag^2 & 6cg^2 & -6a^2g & -12acg & -6c^2g & a^3 & 3a^2c & 3ac^2 & c^3 \\ 2g\alpha_1 & 2g\beta_1 & -2a\alpha_2 & -4\delta_1 & -2c\beta_2 & a^2b & a\gamma_1 & c\gamma_1 & c^2d \\ 2h\alpha_2 & 2h\beta_2 & -2b\alpha_1 & -4\delta_2 & -2d\beta_1 & ab^2 & b\gamma_1 & d\gamma_2 & cd^2 \\ 6bh^2 & 6dh^2 & -6b^2h & -12bdh & -6d^2h & b^3 & 3b^2d & 3bd^2 & d^3 \end{bmatrix} \begin{bmatrix} f_x \\ f_y \\ f_{xx} \\ f_{xy} \\ f_{yy} \\ f_{xxx} \\ f_{xxy} \\ f_{xyy} \\ f_{yyy} \end{bmatrix}.$$

494 where $\alpha_1 = bg + 2ah$, $\alpha_2 = 2bg + ah$, $\beta_1 = dg + 2ch$, $\beta_2 = 2dg + ch$, $\gamma_1 = bc + 2ad$, $\gamma_2 = 2bc + ad$,
 495 and $\delta_1 = (bcg + adg + ach)$, $\delta_2 = (bdg + bch + adh)$.

496 We begin the construction of the moving frame by choosing $\bar{f}_{\bar{x}} = 1$ and $\bar{f}_{\bar{y}} = 0$, which
 497 determines the group parameters $a = (1 - cf_y)/f_x$ and $b = -df_y/f_x$. Direction substitution
 498 then shows that $\bar{f}_{\bar{y}\bar{y}} = Dd^2/f_x^2$, where $D = f_x^2 f_{yy} + f_y^2 f_{xx} - 2f_x f_y f_{xxy}$ was listed in Eq. (4.5)

499 as an invariant of $A(2)$, which is a subgroup of $PSL(3, \mathbb{R})$. Note that D and $\bar{f}_{\bar{y}\bar{y}}$ have the
500 same sign. If $D < 0$, we choose the frame $\bar{f}_{\bar{y}\bar{y}} = -1$ and if $D \geq 0$ we choose $\bar{f}_{\bar{y}\bar{y}} = 1$. Then
501 $d = f_x/|D|^{1/2}$.

502 The frame $\bar{f}_{\bar{y}\bar{y}\bar{y}} = 0$ determines the group parameter $h = \frac{f_{yyy}f_x^3 - 3f_x^2f_yf_{xyy} + 3f_xf_y^2f_{xxy} - f_y^3f_{xxx}}{6|D|^{3/2}}$,
503 while $\bar{f}_{\bar{x}\bar{y}\bar{y}} = 0$ provides $c = \frac{hf_x^2}{dD} - \frac{f_xf_{xy} - f_yf_{xx}}{D}$, and $\bar{f}_{\bar{x}\bar{x}} = 0$ gives $g = \frac{1}{2f_x^2}(f_{xx} + 2c(f_xf_{xy} - f_yf_{xx}) + c^2D)$. In fact, the numerator of the expression for h was another invariant of $A(2)$
504 labelled as E in Eq. (4.5).

505 Having determined the frame, any function of the remaining derivatives $\bar{f}_{\bar{x}\bar{x}\bar{x}}$, $\bar{f}_{\bar{x}\bar{x}\bar{y}}$, and
506 $\bar{f}_{\bar{y}\bar{y}\bar{y}}$, as given in Eq. (5.10), provides invariants. We choose:

$$508 \quad (\bar{f}_{\bar{x}\bar{x}\bar{x}}, \bar{f}_{\bar{x}\bar{x}\bar{y}}, \bar{f}_{\bar{y}\bar{y}\bar{y}}) = \left(\frac{J_1}{D^6}, \frac{J_2}{D^9}, \frac{J_3}{D^3} \right).$$

509 The terms J_1, J_2, J_3 can be written in terms of D and E , together with a polynomial of degree
510 n denoted by P_n .

$$511 \quad J_1 = E^4 + DP_{13}, \quad J_2 = (E^3 + DP_9)^2, \quad J_3 = E^2 - 12DP_5.$$

512 The J_i are polynomials of degree 16, 24, and 8, respectively, and are extremely complicated
513 when written out explicitly. They do have one benefit, though, which is that they all have
514 denominators given by integer powers of D , resolving the ambiguity caused by the sign of
515 D . Therefore, $(D^{18}, J_1^3, J_2^2, J_3^6)$ are all relative invariants of weight 36, and so projecting any
516 subset of them to a sphere yields a third-order invariant signature.

517 J vanishes on generic images: $J = 0$ when $D = E = 0$, which is a codimension 0
phenomenon for images. In particular, $D = E = 0$ at critical points. However, these signatures
can be simplified and made more robust. Their structure suggests considering the combination
 $J_1 - J_3^2$, which obeys:

$$J_1 - J_3^2 = 144D^4P_4.$$

518 As J_1/D^6 and J_3/D^3 are invariant, so is P_4/D^2 . Moreover, the numerator of this new
invariant does not vanish at critical points. It has the structure:

$$P_4 = -4(\det f_{ij})^2 + Q_4,$$

519 where Q_4 is a polynomial of degree 4 that vanishes when $f_x = f_y = 0$. Hence, the relative
520 invariant signature of weight 12 $(D^6, P_4^3, (E^2 - 12DP_5)^2)$ can be projected to S^2 , yielding a
521 projective invariant of images that is singular only when $D = E = P_4 = 0$, which is a codi-
522 mension 1 phenomenon, since $D = E = 0 \Rightarrow P_4 = 0$. In particular, at critical points it tends
523 to $(0, (2\det f_{ij})^6, 0)$, and hence critical points with $\det f_{ij} \neq 0$ have signature value $(0, 1, 0)$.
524 Including J_2 provides a 4-dimensional signature set, but does not change the codimension of
525 the set of bad images.

526 **5.5. Conformal Diffeomorphisms Diff_{con} .** The conformal camera model is well known.
The group of conformal diffeomorphisms is the subgroup of diffeomorphisms (i.e., smooth
functions with smooth inverses) that are angle-preserving:

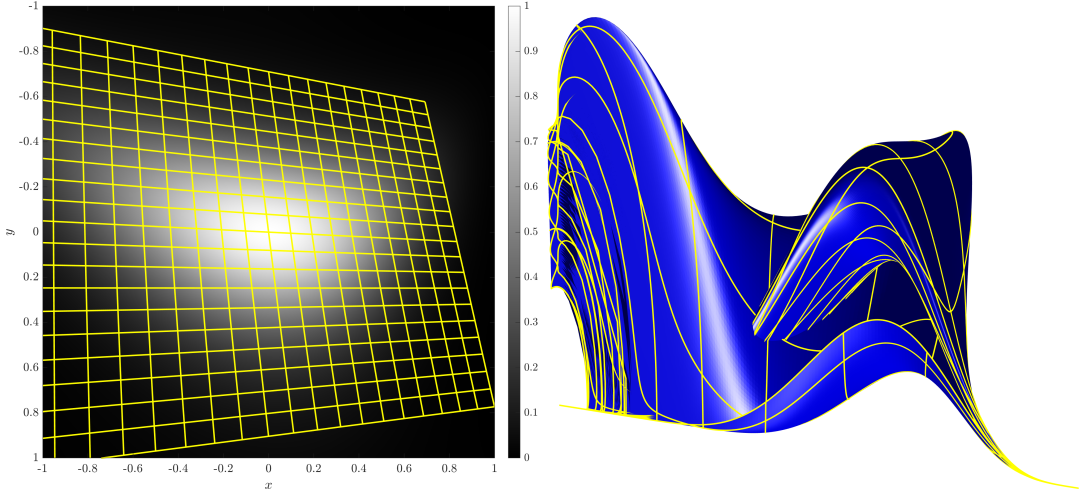


Figure 10. A sample $PSL(3, \mathbb{R})$ transform and 3D signature.

527 (5.11) $\angle(u, v) = \angle(D\phi(x).u, D\phi(x).v),$

528 where $\angle(u, v)$ denotes the angle between tangent vectors u and v based at $x \in \mathbb{R}^2$, $\phi \in \text{Diff}$
 529 and D represents the Jacobian. The group is infinite-dimensional, but still small enough that
 530 images have local differential invariants.

531 The conformal diffeomorphisms provides a particularly nice example of the moving frame
 532 method. Because the group is infinite dimensional, we need to prolong the group action to
 533 the infinite jet space J^∞ with elements of the form $(x, y, f, f_x, f_y, f_{xx}, f_{xy}, f_{yy}, \dots)$.

534 It is convenient to work in the complex variable $z = x + iy$. Without loss of generality, we
 535 can assume $x = y = 0$. We begin the construction of our cross-section by choosing $\bar{x} = \bar{y} = 0$.
 536 Then ψ^{-1} can be represented locally by a Taylor series of the form:

537
$$z = \psi^{-1}(\bar{z}) = c_1\bar{z} + c_2\bar{z}^2 + c_3\bar{z}^3 + \dots,$$

538 where $c_k = a_k + ib_k, k = 1, 2, \dots$. We solve for the parameters a_k, b_k in stages. To find
 539 $c_1 = a_1 + ib_1$ we need two constraints. Differentiating $f(x, y) = \bar{f}(\bar{x}, \bar{y})$ and substituting in
 540 our existing cross-section constraints $\bar{x} = \bar{y} = 0$ gives:

541
$$\begin{aligned} \bar{f}_{\bar{x}} &= f_x x_{\bar{x}} + f_y y_{\bar{x}} = a_1 f_x + b_1 f_y, \\ 542 \bar{f}_{\bar{y}} &= f_x x_{\bar{y}} + f_y y_{\bar{y}} = -b_1 f_x + a_1 f_y. \end{aligned}$$

544 Note that $\bar{x} = \bar{y} = 0$ removes all higher order derivatives from the cross-section equation.
 545 Adding two extra constraints to the cross section, $\bar{f}_{\bar{x}} = 1, \bar{f}_{\bar{y}} = 0$, this system is readily solved
 546 to give:

547
$$a_1 = f_x/(f_x^2 + f_y^2), \quad b_1 = f_y/(f_x^2 + f_y^2).$$

548 We then repeat the process, this time using the second derivative computations. There are two
 549 new parameters, a_2, b_2 , to solve for, but there are three derivatives. We use the cross-section
 550 equations $\bar{f}_{\bar{x}\bar{x}} = 0, \bar{f}_{\bar{x}\bar{y}} = 0$ to solve for a_2 and b_2 , the remaining derivative $\bar{f}_{\bar{y}\bar{y}}$ is then the sole
 551 second-order invariant, which we also saw for the Möbius group:

552 (5.12)
$$\bar{f}_{\bar{y}\bar{y}} = \frac{\bar{f}_{xx} + \bar{f}_{yy}}{\bar{f}_x^2 + \bar{f}_y^2} = \frac{C_1}{\bar{f}_x^2 + \bar{f}_y^2}.$$

553 Continuing in this way, at derivative order n two real group parameters enter: a_n and b_n .
 554 There are $n+1$ independent derivatives of f of order n , so there must be $n-1$ new indepen-
 555 dent invariants at each order. Hence at third order there are two more invariants, using the
 556 constraints $\bar{f}_{\bar{x}\bar{x}\bar{x}} = 0, \bar{f}_{\bar{x}\bar{x}\bar{y}} = 0$, the remaining derivatives are invariant:

(5.13)

557
$$\begin{aligned} \bar{f}_{\bar{x}\bar{y}\bar{y}} &= \frac{1}{(\bar{f}_x^2 + \bar{f}_y^2)^3} [f_y^3 f_{yyy} + f_x^2 f_y f_{yyy} - 2f_y^2 f_{yy}^2 - 2f_{xx} f_y^2 f_{yy} - 4f_x f_{xy} f_y f_{yy} - 2f_x^2 f_{xx} f_{yy} \\ &\quad + f_{xxy} f_y^3 + f_x^2 f_{xxy} f_y - 4f_x f_{xy} f_{xx} f_y + f_x^3 f_{xxx} - 2f_x^2 f_{xx}^2 + f_x^3 f_{xyy}] = \frac{C_2}{(\bar{f}_x^2 + \bar{f}_y^2)^3} \end{aligned}$$

(5.14)

558
$$\begin{aligned} \bar{f}_{\bar{y}\bar{y}\bar{y}} &= \frac{1}{(\bar{f}_x^2 + \bar{f}_y^2)^3} [f_x f_y^2 f_{yyy} + f_x^3 f_{yyy} - 2f_x f_y f_{yy}^2 + 2f_{xy} f_y^2 f_{yy} - 2f_x^2 f_{xy} f_{yy} - f_{xxx} f_y^3 \\ &\quad - f_{xyy} f_y^3 + f_x f_{xxy} f_y^2 + 2f_{xy} f_{xx} f_y^2 - f_x^2 f_{xxx} f_y + 2f_x f_{xx}^2 f_y - f_x^2 f_{xyy} f_y \\ &\quad + f_x^3 f_{xxy} - 2f_x^2 f_{xy} f_{xx}] = \frac{C_3}{(\bar{f}_x^2 + \bar{f}_y^2)^3} \end{aligned}$$

560 Note that the denominators of all three of these equations are the same up to index. We
 561 therefore clear denominators as usual and form the signature using our usual projection tech-
 562 nique:

563 (5.15)
$$\mathcal{I}_{\text{Diff}_{\text{con}}}(f) = \frac{f}{\sqrt{C_1^6 + C_2^2 + C_3^2}}(C_1^3, C_2, C_3)$$

564 This signature is continuous at all (x, y) such that the three quantities are not simultaneously
 565 equal to zero, which occurs when $f_x = f_y = f_{xx} = f_{yy} = 0$, which is a codimension 1
 566 phenomenon for images.

567 An example for the conformal map φ defined through $\varphi^{-1}(z) = \frac{3}{8}(z-2)^2 - \frac{3}{2}$ is
 568 shown in Fig. 11.

569 **5.6. Diff_{vol} and Diff.** Two other infinite-dimensional groups are of interest: the volume-
 570 preserving diffeomorphisms, which act as the space of transformations of an incompressible
 571 fluid, and the full group of planar diffeomorphisms, which are widely-used in image registra-
 572 tion [Younes, 2010]. However, in these cases there are no differential invariant signatures of
 573 greyscale images.

The volume-preserving diffeomorphisms Diff_{vol} are those diffeomorphisms that preserve
 the volume form (area form in 2D). They can be defined by one function of two variables, the

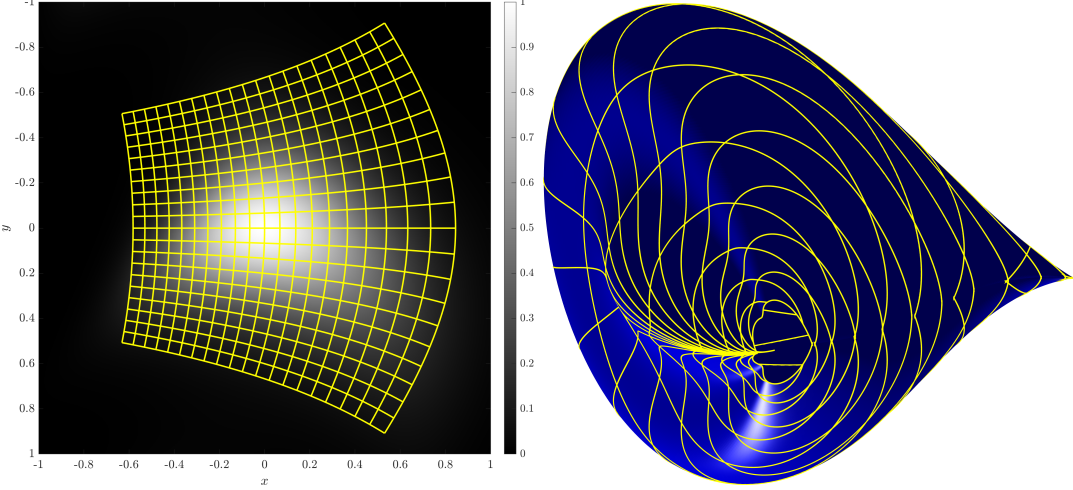


Figure 11. A sample Diff_{con} Transform and 3D signature.

generating function S ; one possibility is $S(x', y')$ where $(x, y) \mapsto (x', y')$ according to:

$$x' = \frac{\partial S}{\partial y'}, \quad y = \frac{\partial S}{\partial x}.$$

574 Consider expanding S in Taylor series. The linear terms in the map are determined from
 575 the quadratic terms in S , which contain 3 group parameters, and act on 2 coordinates, f_x and
 576 f_y . The quadratic terms in the map are determined from the cubic terms in S , which contain
 577 4 group parameters, and act on 3 coordinates, f_{xx} , f_{xy} , and f_{yy} . At order n we have $n+2$
 578 new group parameters acting on $n+1$ coordinates. Thus, barring some exceptional behaviour
 579 in the action, we do not expect any invariants at generic points. This can be confirmed by
 580 considering a small image patch with $f(x, y) = x$. Let $v = \psi_y \partial/\partial_x - \psi_x \partial/\partial_y$ be the generator
 581 of an area-preserving map. The image f transforms to $x + \varepsilon \psi_y(x, y)$ which (by choosing ψ
 582 appropriately) can be any function close to x . At nongeneric points, there can be invariants.
 583 For example, the area enclosed in any level set of f is invariant. At minima or maxima of f ,
 584 this will lead to invariants expressed in terms of the derivatives of f .

585 In the full diffeomorphism group Diff there are no differential invariants using 1 or even
 586 2 colours (colour will be discussed in the Section 6). For example, with $k=2$, for generic f^1 ,
 587 f^2 we can choose a diffeomorphism (i.e., choose local coordinates) so that $f^1 = x$ and $f^2 = y$.

588 **6. Discussion.** The recognition of objects within images as their appearance changes
 589 based on camera motion remains an unsolved problem. In this paper we have used three
 590 different methods of computing differential invariant signatures to identify appropriate signa-
 591 tures for images transformed under the planar Lie groups that are of interest for this question.
 592 The resulting three-dimensional signatures are not always complete, but they are relatively
 593 fast to compute. However, there are some issues that arise with turning this into a practical
 594 method.

595 The first is a standard issue for images: producing a computationally robust method
 596 of numerically approximating derivatives and hence invariants is not trivial, particularly for

597 the higher-orders, where noise and rounding errors can dominate. There are three primary
 598 considerations: noise and texture; flat areas, where the derivatives are all identically zero;
 599 and the fact that conventional numerical differentiation is not well-posed [Florack et al.,
 600 1993]. Some considerations of these points and some potential approaches to solving them for
 601 practical implementations are considered by Calabi et al. [1998] and Florack et al. [1993], but
 602 the question of how to create a full and effective method of computing numerical derivatives
 603 for images remains open. Practical approaches to using the signatures identified in this paper
 604 for real-world images will be considered in future work.

605 The second problem is that there are hidden symmetries within the lattice of groups we
 606 consider. For example, the relation $SA(2) \subset \text{Diff}_{\text{vol}}$ acts as an obstruction to $SA(2)$, since many
 607 of the invariants of $SA(2)$ are also invariant under the larger group. While there will be more
 608 invariants for the smaller group, care needs to be taken to check that the set chosen are unique
 609 to that group. The same issue arises with $A(2)$, even though $A(2)$ is not even a subgroup of
 610 Diff_{vol} .

611 It might be hoped that colour information can help. The formulation we provided in the
 612 introduction considered k channels of information, but so far we have considered only greyscale
 613 images ($k = 1$). Most real images are three-channel colour (RBG), and multi-spectral images
 614 can have hundreds of channels of measurement. It is therefore natural to consider whether
 615 this information is useful for the computation of invariants, in particular by allowing lower-
 616 order derivatives to form a suitable signatures. However, in practice the situation is more
 617 complicated than it first appears because the information in the channels is not independent:
 618 colour is built by the intensities in the three channels, and so there is correlation between
 619 them.

620 For $E(2)$, for $k \geq 2$, first derivatives suffice, but for both $SA(2)$ and $A(2)$ the hidden
 621 symmetry noted above mean that there are no signatures with only first derivatives.

The picture is more positive for the infinite-dimensional groups. For Diff_{con} , first-order
 signature sets are possible for $k \geq 2$ colours. They are formed from the relative invariants
 $(f_x^j + if_y^j)(f_x^m - if_y^m)$ of weight 2 (where f^j is the j th colour channel). We illustrate this
 using the Hopf fibration for $k = 2$. The weight 2 relative invariant

$$J = (2(f_x^1 + if_y^1)(f_x^2 - if_y^2), \|\nabla f^1\|^2 - \|\nabla f^2\|^2)$$

622 obeys $\|J\|^2 = \|\nabla f^1\|^2 + \|\nabla f^2\|^2$, hence projecting to the unit sphere shows that $(f^1, f^2, J/\|J\|)$
 623 provides a 4-dimensional signature set that is singular only when $\nabla f^1 = \nabla f^2 = 0$, a co-di-
 624 mension 2 phenomenon for images. For Diff_{vol} extra channels mean that different invariants
 625 now exist: there are $k(k-1)/2$ first-order invariants $\nabla f^i \times \nabla f^j$. Then the three-dimensional
 626 signature $(f^1, f^2, \nabla f^1 \times \nabla f^2)$ determines (generically and locally) the image up to an area-
 627 preserving map. We can choose the area-preserving map so that $f^1 = x$. The remaining
 628 freedom is of the area-preserving maps that preserve x : these are the shears $y \mapsto y + g(x)$.
 629 The signature for each fixed x now gives (f^2, f_y^2) . This is the standard signature curve for the
 630 group of translations in y . Thus, f^2 is determined by the signature up to a translation in y ,
 631 i.e., an area-preserving map.

632 In the full diffeomorphism group Diff there are no differential invariants using 1 or 2
 633 colours. For example, with $k = 2$, for generic f^1, f^2 we can choose a diffeomorphism (i.e.,
 634 choose local coordinates) so that $f^1 = x$ and $f^2 = y$. We therefore take $k \geq 3$. This provides

635 the first-order relative invariants of weight 1 $\nabla f^i \times \nabla f^j$, and hence a first-order signature.
 636 However, a zeroth-order signature set is possible: (f^1, \dots, f^k) , the image of the image. It is
 637 (locally and generically) complete. We can choose coordinates so that $f^1 = x$ and $f^2 = y$;
 638 then the signature locally determines f^3, \dots, f^k as functions of f^1 and f^2 , i.e., the image.

639 Putting all of this information together, Table 3 summarises one of the most important
 640 parameters of differential invariant signatures for the transformation groups that we have
 641 considered, namely the highest order of derivative of the image that is needed. None of
 642 the groups need more than third-order differentiation, and usually less, especially for colour
 643 images.

\mathcal{G}	Degree		
	$k = 1$	$k = 2$	$k = 3$
$SE(2)$	2	1	1
$E(2)$	2	1	1
$Sim(2)$	2	1	1
$SA(2)$	2	2	2
$A(2)$	3	2	2
$PSL(2, \mathbb{C})$	3	3	3
$PSL(3, \mathbb{R})$	3	2	2
Diff_{vol}	—	1	1
Diff_{con}	3	1	1
Diff	—	—	0

Table 3

Degree (order of highest derivative of f) needed to construct a differential invariant signature of f as a function of the group \mathcal{G} and the number of colours k of f . The entry ‘—’ indicates that there is no differential invariant signature in that case.

644 In future work we will seek the underlying mathematical structure that we have not fully
 645 exposed. For example, all of the second-order differential invariants of $E(2)$ play known roles
 646 in geometric analysis:

- $f_x^2 + f_y^2 = \|\nabla f\|^2$ is the Lagrangian density for the Laplacian;
- $f_{xx} + f_{yy}$ is the Laplacian, which plays a key role in Euclidean and conformal geometry;
- $f_{xx}f_x^2 + 2f_{xy}f_xf_y + f_{yy}f_y^2$ is the ‘infinity-Laplacian’;
- $f_{xx}f_x^2 + 2f_{xy}f_xf_y + f_{yy}f_y^2$ is also a Lagrangian density for $-2(f_{xx}f_{yy} - f_{xy}^2)$, which arises in the Monge–Ampère equations and can be written in terms of the final second-order invariant as $-2(f_{xx}f_{yy} - f_{xy}^2) = 2f_{xy}^2 - f_{xx}^2 - f_{yy}^2$

653 Functions of these invariants are invariants or relative invariants for many groups that
 654 contain $E(2)$, such as those that we have considered in this paper. We will consider this
 655 further in future work.

656 Function D from Eq. (4.5), which appeared in $SE(2)$, $SA(2)$ and $PSL(3, \mathbb{R})$, is also
 657 known as the Bateman equation [Andriopoulos et al., 2009], and is linked to the Hodograph
 658 transformation [Rosenhaus, 1988].

659 References.

660 K. Andriopoulos, S. Dimas, P.G.L. Leach, and D. Tsoubelis. On the systematic approach

- 661 to the classification of differential equations by group theoretical methods. *Journal of*
 662 *Computational and Applied Mathematics*, 230:224–232, 2009.
- 663 Raman Arora, Yu Hen Hu, and Charles Dyer. Estimating correspondence between multiple
 664 cameras using joint invariants. In *Proceedings of the IEEE International Conference on*
 665 *Acoustics, Speech and Signal Processing*, pages 805–808, 2009.
- 666 Herbert Bay, Andreas Ess, Tinne Tuytelaars, and Luc Van Gool. SURF: Speeded up robust
 667 features. *Computer Vision and Image Understanding*, 110(3):346–359, 2008.
- 668 James Benn, Stephen Marsland, Robert McLachlan, Klas Modin, and Olivier Verdier. Cur-
 669 rents and finite elements as tools for shape space. *Journal of Mathematical Imaging and*
 670 *Vision*, 61(8):1197–1220, 2019.
- 671 Charles L Bouton. Some examples of differential invariants. *Proceedings of the American*
 672 *Mathematical Society*, pages 313–322, 1898.
- 673 Eugenio Calabi, Peter J Olver, Chehrzad Shakiban, Allen Tannenbaum, and Steven Haker.
 674 Differential and numerically invariant signature curves applied to object recognition. *Inter-*
 675 *national Journal of Computer Vision*, 26(2):107–135, 1998.
- 676 É. Cartan. La méthode du repère mobile, la théorie des groupes continus, et les espaces
 677 généralisés. In *Exposes de Geometrie*, volume 5. Hermann, Paris, 1935.
- 678 É. Cartan. Les problèmes d'équivalence. In *Oeuvres Complètes*, volume 2, pages 1311–1334.
 679 Gauthiers-Villars, Paris, 1952.
- 680 A. Cayley. An introductory memoir on quantics. *Philosophical Transactions of the Royal*
 681 *Society of London*, 144:244–258, 1845.
- 682 Arthur Cayley. On linear transformations. *Cambridge and Dublin Mathematical Journal*, 1:
 683 104–122, 1846.
- 684 Olivier Faugeras. Cartan's Moving Frame Method and its Application to the Geometry and
 685 Evolution of Curves in the Euclidean, Affine and Projective Planes. In *Applications of*
 686 *Invariance in Computer Vision*, volume 825, pages 9–46, 1994.
- 687 Mark Fels and Peter J Olver. On relative invariants. *Mathematische Annalen*, 308(4):701–732,
 688 1997. doi: 10.1007/s002080050097.
- 689 S. Feng, Irina A Kogan, and Hamid Krim. Classification of curves in 2D and 3D via affine
 690 integral signatures. *Acta Applicandae Mathematicae*, 109:903–937, 2010.
- 691 L. M.J. Florack, B. M. Ter Haar Romeny, J. J. Koenderink, and M. A. Viergever. Cartesian
 692 differential invariants in scale-space. *Journal of Mathematical Imaging and Vision*, 3(4):
 693 327–348, 1993. doi: 10.1007/BF01664793.
- 694 Jan Flusser, Jaroslav Kautsky, and Filip Šroubek. Implicit Moment Invariants. *International*
 695 *Journal of Computer Vision*, 86(1):72–86, 2009. doi: 10.1007/s11263-009-0259-4.
- 696 Jean-Paul Gauthier, Fethi Smach, Cedric Lemaître, and Johel Miteran. Finding invariants
 697 of group actions on function spaces, a general methodology from non-Abelian harmonic
 698 analysis. In *Mathematical Control Theory and Finance*, pages 161–186. Springer, Berlin,
 699 2008.
- 700 Faouzi Ghorbel. A complete invariant description for gray-level images by the harmonic
 701 analysis approach. *Pattern Recognition Letters*, 15:1043–1051, 1994.
- 702 A. González-López, N. Kamran, and P. J. Olver. Lie algebras of vector fields in the real plane.
 703 *Proceedings of the London Mathematical Society*, 64(3):339–368, 1992.
- 704 P Gros and L Quan. Projective Invariants for Vision. Technical Report RT 90 IMAG-15LIFIA,

- 705 INRIA, 1992.
- 706 C. E. Hann and Mark Hickman. Projective curvature and integral invariants. *Acta Applicandae
707 Mathematicae*, 74(2):177–193, 2002. doi: 10.1023/A:1020617228313.
- 708 Mark Hickman. Geometric Moments and their Invariants. *Journal of Mathematical Imaging
709 and Vision*, 44:223–235, 2011. doi: 10.1007/s10851-011-0323-x.
- 710 Daniel J Hoff and Peter J Olver. Extensions of Invariant Signatures for Object Recog-
711 nition. *Journal of Mathematical Imaging and Vision*, 45(2):176–185, 2013. doi: 10.1007/
712 s10851-012-0358-7.
- 713 M.K. Hu. Visual pattern recognition by moment invariants. *IRE Transactions on Information
714 Theory*, IT-8:179–187, 1962.
- 715 Evelyne Hubert. Differential invariants of a lie group action: syzygies on a generating set.
716 *Journal of Symbolic Computation*, 44(4):382–416, 2009.
- 717 Evelyne Hubert and Peter J Olver. Differential invariants of conformal and projective surfaces.
718 *SIGMA*, 2007. URL <http://www.emis.ams.org/journals/SIGMA/2007/097/sigma07-097.pdf>.
- 719 Ramakrishna Kakarala. The bispectrum as a source of phase-sensitive invariants for Fourier
720 descriptors: a group-theoretic approach. *Journal of Mathematical Imaging and Vision*, 44:
721 341–353, 2012.
- 722 David G Kendall. A Survey of the Statistical Theory of Shape. *Statistical Science*, 4(2):
723 116–120, 1989. doi: 10.1214/ss/1177012589.
- 724 Irina A Kogan and Peter J Olver. Invariants of objects and their images under surjective
725 maps. *Lobachevskii Journal of Mathematics*, 36:260–285, 2015.
- 726 H Kraft and C Procesi. Classical invariant theory, a primer, 2002.
- 727 Reiner Lenz. *Group Theoretical Methods in Image Processing*. Springer, Berlin, 1990.
- 728 E. Li, H. Mo, D. Xu, and H. Li. Image projective invariants. *IEEE Transactions on Pat-
729 tern Analysis and Machine Intelligence*, 41(5):1144–1157, 2019. doi: 10.1109/TPAMI.2018.
730 2832060.
- 731 S. Lie. Über differentialinvarianten. *Mathematische Annalen*, 24(4):537–578, 1884.
- 732 D.E. Littlewood. Invariant theory, tensors and group characters. *Philosophical Transactions
733 of the Royal Society of London, Series A*, 239(807):305–356, 1944.
- 734 Siddharth Manay, Daniel Cremers, Byung-Woo Hong, Anthony Yezzi, and Stefano Soatto. In-
735 tegral invariants for shape matching. *IEEE Transactions on Pattern Analysis and Machine
736 Intelligence*, 28(10):1602–1618, 2006. doi: 10.1109/TPAMI.2006.208.
- 737 Stephen Marsland and Robert McLachlan. Möbius invariants of shapes and images. *SIGMA*,
738 12(80), 2016.
- 739 Jan Modersitzki. *Numerical Methods for Image Registration*. Oxford University Press, Oxford,
740 2003.
- 741 J.L. Mundy and A. Zisserman. *Geometric Invariance in Computer Vision*. MIT Press, Cam-
742 bridge, Mass, USA, 1992.
- 743 Renato MP Negrinho and Pedro MQ Aguiar. Shape Representation via Elementary Symmetric
744 Polynomials: A Complete Invariant Inspired by the Bispectrum. In *IEEE International
745 Conference on Image Processing*, 2013.
- 746 Peter J Olver. *Equivalence, Invariants and Symmetry*. Cambridge University Press, Cam-
747 bridge, 1995.

- 749 Peter J Olver. *Classical Invariant Theory*. Cambridge University Press, Cambridge, 1999.
- 750 Peter J Olver. Joint Invariant Signatures. *Foundations of Computational Mathematics*, 1(1):
751 3–68, 2001. doi: 10.1007/s10208001001.
- 752 Peter J Olver. A Survey of Moving Frames. In *Computer Algebra and Geometric Algebra with
753 Applications*, pages 105–138. Springer, Berlin, 2005.
- 754 Peter J Olver. Generating differential invariants. *Journal of Mathematical Analysis and
755 Applications*, 333(1):450–471, 2007. doi: 10.1016/j.jmaa.2006.12.029.
- 756 G.A. Papakostas, D.E. Koulouriotis, E.G. Karakasis, and V.D. Tourassis. Moment-based
757 local binary patterns: A novel descriptor for invariant pattern recognition applications.
758 *Neurocomputing*, 99:358–371, 2013. doi: 10.1016/j.neucom.2012.06.031.
- 759 Boyd C Patterson. The Differential Invariants of Inversive Geometry. *American Journal of
760 Mathematics*, 50(4):553–568, 1928.
- 761 Xavier Pennec, Stefan Sommer, and Tom Fletcher, editors. *Riemannian Geometric Statistics
762 in Medical Image Analysis*. Academic Press, Cambridge, Mass, USA, 2019.
- 763 B. Srinivasa Reddy and B.N. Chatterji. An FFT-Based Technique for Translation, Rotation,
764 and Scale-Invariant Image Registration. *IEEE Transactions on Image Processing*, 5(8):
765 1266–1271, 1996.
- 766 V. Rosenhaus. Groups of invariance and solutions of equations determined by them. *Algebras,
767 Groups and Geometries*, 5:137–150, 1988.
- 768 Fethi Smach, Cedric Lemaître, Jean-Paul Gauthier, Johel Miteran, and Mohamed Atri. Gen-
769 eralized Fourier Descriptors with Applications to Objects Recognition in an SVM Con-
770 text. *Journal of Mathematical Imaging and Vision*, 30(1):43–71, 2007. doi: 10.1007/
771 s10851-007-0036-3.
- 772 Tomáš Suk and Jan Flusser. Point-based projective invariants. *Pattern Recognition*, 33(2):
773 251–261, 2000. doi: 10.1016/S0031-3203(99)00049-7.
- 774 Tomáš Suk and Jan Flusser. Projective Moment Invariants. *IEEE Transactions on Pattern
775 Analysis and Machine Intelligence*, 26(10):1364–1367, 2004.
- 776 A. Tresse. Sur les invariants différentiels des groupes continus de transformations. *Acta
777 Mathematica*, 10(1):1–88, 1984.
- 778 Jacek Turski. Geometric Fourier Analysis of the Conformal Camera for Active Vision. *SIAM
779 Review*, 46(2):230–255, 2004. doi: 10.1137/S0036144502400961.
- 780 Jacek Turski. Computational harmonic analysis for human and robotic vision systems. *Neu-
781 rocomputing*, 69(10-12):1277–1280, 2006. doi: 10.1016/j.neucom.2005.12.091.
- 782 L Van Gool, T Moons, E Pauwels, and A Oosterlinck. *Semi-differential invariants*, pages
783 157–192. MIT Press, Cambridge, Mass, USA, 1992.
- 784 L Van Gool, T Moons, E J Pauwels, and A Oosterlinck. Vision and Lie’s approach to invari-
785 ance. *Image and Vision Computing*, 13:259–277, 1995. doi: 10.1016/0262-8856(95)99715-D.
- 786 Oswald Veblen. Differential invariants and geometry. *International Congress on Mathematics*,
787 1:181–189, 1929.
- 788 Jeffrey Wood. Invariant pattern recognition: A review. *Pattern Recognition*, 29(1):1–17, 1996.
789 doi: 10.1016/0031-3203(95)00069-0.
- 790 L Younes. *Shapes and Diffeomorphisms*. Springer, New York, USA, 2010.
- 791 Suzhi Zhang, Yuhong Wu, and Jun Chang. Survey of image recognition algorithms. In
792 *2020 IEEE 4th Information Technology, Networking, Electronic and Automation Control*

- 793 Conference (ITNEC), pages 542–548, 06 2020. doi: 10.1109/ITNEC48623.2020.9084972.
- 794 Xinhua Zhang and Lance R. Williams. Euclidean invariant recognition of 2D shapes using
795 histograms of magnitudes of local Fourier-Mellin descriptors. *Proceedings of the IEEE*
796 Winter Conference on Applications of Computer Vision, pages 303–311, 2019. doi: 10.
797 1109/WACV.2019.00038.